Paleogeographic position of the central Dodecanese Islands, southeastern Greece: The push-pull of Pelagonia

B. Grasemann, D.A. Schneider, K. Soukis, Vincent Roche, B. Hubmann

Paleogeographic position of the central Dodecanese, western Greece: the push-pull of the Pelagonian

B. Grasemann[1], D.A. Schneider[2], K. Soukis[3], V. Roche[4], B. Hubmann[5]

[1)] Department of Geology, University of Vienna, Austria

[2)] Department of Earth and Environmental Sciences, University of Ottawa, Canada

[3)] Faculty of Geology and Geoenvironment, National and Kapodistrian University of Athens, Greece

[4)] UPMC Institut des Sciences de la Terre Paris, Sorbonne Université, France

[5)] Institute for Earth Sciences, University of Graz, Austria

Abstract

The paleogeographic position having a first order influence on the Cenozoic tectonic history of the central Dodecanese islands at the transition between the Aegean and Anatolian plates plays a considerable role in understanding the link between both geologically different domains.

In this study, we investigate the tectonic history of the central Dodecanese and the general correlation with the Aegean and western Anatolian focusing on the poorly studied island of Kalymnos and Telendos. Three different major tectonic units were mapped on both islands from bottom to top: (i) The Kefala Unit consists of Late Paleozoic fossil-rich limestones, which have been deformed into a SE-vergent fold-and-thrust belt sealed by an up to 200 m-thick wildflysch-type olistostrome with tens of meters-scale marble and ultramafic blocks. (ii) The Marina Basement Unit consists of a Variscan amphibolite facies basement with garnet mica schists, quartzites and amphibolites. (iii) Verrucano-type formation violet shales and Mesozoic unmetamorphosed limestones form the Marina Cover Unit. Correlation of these units with other units in the Aegean suggest that Kalymnos is paleogeographically located at the southern margin of the Pelagonian domain, and therefore, in a structurally upper tectonic position during the Paleogene alpine orogeny.

New white mica $^{40}Ar/^{39}Ar$ ages confirm the Carboniferous deformation of the Marina Basement Unit followed by a Triassic thermal signal. Single grain white mica $^{40}Ar/^{39}Ar$ ages from pressure solution cleavage of the newly defined Telendos Thrust suggest that the Marina Basement Unit was thrusted towards the north on top of Kefala Unit in the Paleocene. Located at a tectonically upper position, the units exposed in the central Dodecanese escaped subduction and the syn-orogenic high-pressure metamorphism. However, these units were affected by post-orogenic extension and the contact between the Marina Basement Unit and the non-metamorphic Marina Cover Unit has been reactivated by the cataclastic top-to-SSW low-angle Kalymnos Detachment. Zircon (U-Th)/He ages from the Kefala and Marina Basement units are ca. 30 Ma, indicating exhumation and cooling below the Kalymnos Detachment started in the Oligocene. Conjugate brittle high-angle normal fault systems, which

resulted in the formation of four major WNW-ESE trending graben systems on Kalymnos, localized mainly in the Marina Cover Unit, probably rooting into the mechanically linked Kalymnos Detachment. Since Oligo-Miocene extension in the northern Dodecanese records top-to-NNE and the Kalymnos Detachment a top-to-SSW kinematics, we suggest that back-arc extension in the whole Aegean realm and transition to the Anatolian plate is bivergent.

Introduction

Continuous subduction of lithosphere containing continental blocks below Eurasia started in the Cretaceous leading to the formation of the Hellenides and Taurides orogens (e.g., Jacobshagen et al., 1978; Bonneau, 1984; van Hinsbergen et al., 2005a; Brunn and Faccenna, 2008). Both orogens are composed of assorted nappe sequences, which have been derived from distinctive paleogeographic settings and which have experienced different Cenozoic tectono-metamorphic histories characterized by syn-orogenic subduction/exhumation overprinted by post-orogenic extension to various degrees (Jolivet and Brun, 2010; Ring et al., 2010). Nevertheless, the correlation of the paleogeographic position, the stratigraphy and the tectono-metamorphic history of these nappe sequences between the Hellenides and Taurides is often equivocal (Dürr et al., 1978; Bonneau, 1984; Papanikolaou and Demirtasli, 1987; Robertson et al., 1991; Papanikolaou, 1997; Göncüoğlu et al., 1997; Ring et al., 1999a; Jolivet et al., 2004; Roche et al., 2019).

The geodynamics of the Aegean-Anatolian transition zone is furthermore of great importance because various tomographic models have demonstrated a first-order slab tear below this region (Piromallo and Morelli, 2003; Dilek and Altunkaynak, 2009; Berk Biryol et al., 2011; Salaün et al., 2012; Jolivet et al., 2013). It has been suggested that this Subduction-Transform-Edge-Propagator fault could have caused differential finite rates of back-arc extension (Kissel and Laj, 1988; van Hinsbergen et al., 2005b) and if mechanically linked with the crust may result in in transfer zones of distributed brittle/ductile deformation (Sternai et al., 2014; Jolivet et al., 2021). Western Anatolia is dominated by W-E striking Cenozoic detachment faults, which are associated with domal uplift, exhumation of the Menderes Core Complex and the formation of asymmetric supra-detachment basins (Hetzel et al., 1995; Bozkurt and Oberhänsli, 2001; Gessner et al., 2001). During the Oligocene-Miocene, the Cyclades experienced back-arc extension leading to the formation of Cordilleran-type metamorphic core complexes below several crustal-scale low-angle normal fault systems (Lister et al., 1984; Labrousse et al., 2016). The differential extensional strain between Menderes and the Cycladic core complexes may have been accommodated by tranfer zones, e.g. the NE-SW striking transtensional İzmir-Balıkesir Transfer Zone (Sözbilir et al., 2011; Uzel et al., 2015) or the West Anatolian Transfer Zone (Gessner et al., 2013; Jolivet et al., 2015). Ring et al. (2017) highlighted the fact that the Aegean-Anatolia plate

boundary transition zone spatially coincides with a corridor of relatively old fission-track ages, which were not reset during Miocene tectonism. Fault-slip derived strain axes supported by geodetic data and earthquake focal solutions (Kahle et al., 1999; McClusky et al., 2000; Aktug et al., 2009) suggest a sinistral wrench component that was superimposed on the regional NNE-SSW extension (Ring et al., 2017).

Recently, Roche et al. (2018; 2019) focused on the geology of the northern Dodecanese and showed, despite the complexity involved in the Aegean-Anatolian transition zone, comparable tectonic units exposed on the islands of Fourni, Arki, Lipsi and Leros, linking the geology of the Cyclades with the geology of the Menderes Massif. Most importantly, the authors demonstrated that NNE-SSW extension is predominantly accommodated along top-to-NNE low-angle normal faults. Interestingly, no clear evidence of a large-scale strike-slip fault systems that is expected above a slab tear has been documented. Roche et al. (2019) concluded that there is a gradient in finite extension accommodating the left-lateral displacement imposed by the faster slab retreat south of the Aegean Sea than of the Menderes Massif (Gessner et al., 2013). The different pattern of crustal extension, asymmetrical in the eastern Aegean Sea, but symmetrical in the Cyclades and in the Menderes Massif, may be related to the mantle flow induced by the slab tear in the transfer zone (Jolivet et al., 2015).

In this work we follow Roche et al. (2019) and extend the geological observations further to the south in the central Dodecanese islands of Kalymnos and Telendos (Fig. 1). Although, some of the exposed units can be correlated with the northern Dodecanese, we demonstrate that all rock units on Kalymnos were paleogeographically located further to the N and belong to a structurally higher tectonic unit. Our new geochronological and structural data show that Variscan basement rocks have been thrust towards the north along the newly defined Telendos Thrust in the Paleogene and were exhumed below the Oligocene top-to-SSW Kalymnos Detachment. Our new observations together with recent work in the northern Dodecanese suggest that the whole Aegean-Menderes domain experienced Oligocene-Miocene bivergent extension.

Geological setting in the Aegean-Anatolian transition zone

In the Aegean, Cretaceous closure of the Vardar ocean, which resulted from the convergence between Adria (Hellenides) and Eurasia (Rhodope),was followed by Cenozoic subduction and nappe stacking of the Pelagonian, Pindos, Gavrovo-Tripolitza, Phyllite-Quartzite and Ionian units (Jacobshagen et al., 1978; Sengör and Yilmaz, 1981; Bonneau, 1984). In the Cyclades, the Cycladic Blueschist Unit (CBU) is considered to be an Eocene high-pressure metamorphic equivalent of the Pindos Unit (Blake et al., 1981; Bonneau, 1984; Papanikolaou, 1997; Jolivet et al., 2003; Brun and Faccenna, 2008; Jolivet and Brun, 2010; Ring et al., 2010). The CBU is overlain by the Pelagonian Unit or Upper Unit (Fig. 2), which consists of ophiolitic material obducted over a pre-Alpine continental crystalline basement and its

Paleozoic-Mesozoic sedimentary cover, which partly experienced Late Cretaceous low-pressure/high-temperature metamorphism (Patzak et al., 1994). The CBU is underlain by either the Variscan Cycladic Basement Unit (Dürr et al., 1978; Papanikolaou, 1997; Jolivet and Brun, 2010; Ring et al., 2010) or the Basal Unit, which is a thick marble sequence exposed in several tectonic windows and is considered to be a lateral equivalent of the Gavrovo-Tripolitza Unit (Dürr et al., 1978, Papanikolaou, 1997; Ring et al., 2001). During the Oligocene-Miocene, the nappe stack experienced back-arc extension leading to the formation of Cordilleran-type metamorphic core complexes below several crustal-scale low-angle normal fault systems (Lister et al., 1984; Labrousse et al., 2016). Apart from a debated South Cycladic Shear Zone or South Cycladic Detachment System (Baldwin and Lister, 1998; Forster and Lister, 1999; Ring et al., 2011; Huet et al., 2009; Poulaki et al., 2019), extension has been considered to be mainly asymmetric localizing along the top-to-N/NE North Cycladic (Jolivet et al., 2010) and Naxos-Paros Detachment System (Gautier et al., 1993). However, the discovery of other coeval low-angle normal faults with top-to-S/SW kinematics like the West Cycladic Detachments System (Grasemann et al., 2012) or the Santorini Detachment System (Schneider et al., 2018) have shown that extension in the Cyclades is bivergent.

In Crete, which belongs to the External Hellenides, Cycladic-equivalent units are exposed in an Upper Nappe System (Tripolitza, Pindos, Uppermost Unit/Pelagonian) where nappe stacking occurred during the Oligocene-Miocene (Creutzburg and Seidel, 1975; Le Pichon and Angelier, 1979; Bonneau, 1984). Separated by the Cretan Detachment (Fassoulas et al., 1994; Jolivet et al., 1996; Ring et al., 2001; Grasemann et al., 2019), a Lower Nappe System consists of the Plattenkalk/Ionian Unit and the Phyllite-Quartzite Unit, which record Triassic closure of the Paleotethys during the Eo-Cimmerian event (Şengör et al., 1984a; Zulauf et al., 2018). The Lower Nappe System experienced subduction-related late Oligocene to early Miocene high-pressure/low-temperature metamorphism (Creutzburg et al., 1977; Seidel et al., 1982; Jolivet et al., 1996). The Ionian, Tripolitza and Pindos units have been correlated with the nappe systems in the southern Dodecanese on Karpathos and Rhodes (Aubouin and Dercourt, 1970; Mutti et al., 1970; Bonneau, 1984; Koepke et al., 2002; Lekkas et al., 2002). Recently, Cordey and Quillévéré (2020) showed that ophiolites in the uppermost structural level on Karpathos record Early Cretaceous ages and therefore should not be correlated with the Pindos Unit or the ophiolites of Cyprus or Syria, but rather with the Lycian Nappes of Turkey.

In western Anatolia, the Menderes Massif is a bivergent metamorphic core complex, which exhumed in several stages below three detachment systems that operated throughout the Oligo-Miocene with opposing sense of shear (Hetzel et al., 1995; Gessner et al., 2001; Bozkurt et al., 2011; Heineke et al., 2019). The metamorphic rocks of the central Menderes Massif consist of four major nappes (Ring et al., 1999b) that were stacked during late Cretaceous to Eocene subduction along the Izmir-Ankara suture zone (Şengör et al., 1984b; Bozkurt and Oberhänsli, 2001; van Hinsbergen et al.,

2010; Gessner et al., 2013). The massif is overlain in the south by the Ören Unit (Pourteau et al., 2010), consisting of Mesozoic to Eocene high-pressure/low-temperature metasediments (Fig. 2) (Rimmelé et al., 2005) and probably correlates with the Afyon zone to the north (Pourteau et al., 2013). Stratigraphic relationships bracket the high-pressure/low-temperature metamorphic event in a latest Cretaceous to Eocene interval (Rimmelé et al., 2003; Ring and Layer, 2003) and $^{40}Ar/^{39}Ar$ ages on phengite yield dates of ca. 67-62 Ma for carpholite-bearing assemblages from the Afyon zone and ca. 63-59 Ma from rocks of the Ören Unit (Pourteau et al., 2013). The Ören Unit corresponds to the lower high-pressure/low-temperature part of the Lycian Nappes (Bernoulli et al., 1974), characterized by thrust slices of Paleozoic to Paleocene sedimentary rocks capped by ophiolites that correlate with the Izmir-Ankara ophiolites north and southwest of the Menderes Massif (Okay, 1989; Collins and Robertson, 1997; Rimmelé et al., 2003, 2005; Candan et al., 2005). In the west, Eocene blueschist and eclogite facies rocks occur between the Menderes Massif and the Lycian Nappes/Ören Unit and can be correlated with the CBU (Candan et al., 1997; Oberhänsli et al., 1997, 1998; Ring et al., 1999b). The Upper Cycladic Blueschist Nappe is mainly composed of a Triassic to Upper Cretaceous metasedimentary series overlain by eclogite blocks embedded in a pelitic epidote-blueschist matrix northwest of the Menderes Massif (Fig. 2) (for a more complete tectono-stratigraphic sequence of the eastern Mediterranean see Roche et al., 2019).

The tectonic units in the northern Dodecanes have been recently studied in detail and their correlation may link the geology of the Cyclades with western Anatolia (Roche et al., 2018; 2019; Çetinkaplan et al., 2020). Two major tectonic units can be distinguished: (i) The high-pressure/low-temperature Temenia Unit (Dürr et al., 1978; Franz and Okrusch, 1992; Franz et al., 2005) is composed of metapelites and marbles with minor metabasite and can be correlated with the CBU (Roche et al., 2018), or more specifically with the Lower Cycladic Blueschist Nappe (Fig. 2) (Grasemann et al., 2018), which has experienced pressures ~8-10 kbar and temperatures ~400-450°C. This is in contrast to the Upper Cycladic Blueschist Nappe with higher-pressure blueschist and eclogite conditions reaching ~550°C and 20 kbar on Syros, Sifnos and Sikinos (Fig. 2). (ii) The Marina Unit consists of a Variscan metamorphic basement and a sedimentary cover composed of Permo-Triassic siliciclastic Verrucano-type formation sediments and Mesozoic limestones (Fig. 2) (Dürr et al., 1978; Franz and Okrusch, 1992; Franz et al., 2005). With regard to lithologies and paleogeographical affinities, the cover has many similarities with the Lycian Nappes that belong to the northern margin of the Pelagonian domain (Roche et al., 2019). Both units are juxtaposed by a syn-orogenic low-angle extensional detachment with a top-to-NE kinematics, overprinted and partly cut by a more brittle post-orogenic detachment systems (Thymanea Detachment), reminiscent of the Miocene exhumation of metamorphic domes during back-arc extension in the Cyclades (Roche et al., 2018).

Interestingly, Kalymnos, which lies in the central Dodecanese, has attracted so far relatively little attention and the kinematics of the emplacement of the different tectonic units are unknown (Triantaphyllis and Karfakis, 1994). In marked contrast to the northern Dodecanes, where the lower Temenia Unit records high-pressure/low-temperature metamorphism, the tectonically lowermost unit on Kalymnos records only very low-grade greenschist facies metamorphism (Dürr et al., 1978) and consists of Upper Paleozoic fossiliferous limestones/marbles, schists and quartzites (Fig. 2) (Christodoulou, 1970; Dounas et al., 1983). Similar species of Permian fusulinids have been described from similar fauna in the Southern Alps, Urals and Central Asia (Kahler, 1987). The structurally upper unit on Kalymnos shows many similarities with the Marina Unit in the northern Dodecanese, comprised of amphibolites, quartzitic garnet mica schists and sparse interlayered marbles (Fig. 2) (Dürr, 1986). Amphibole and muscovite K-Ar dating of the basement rocks yield ages between 320-200 Ma broadly suggesting Variscan metamorphism partly overprinted by an early Alpine event (Seidl et al., 1982; Franz et al., 2005). The rocks experienced pre-Alpine amphibolite facies metamorphic conditions with no indication of a high-pressure/low-temperature Alpine overprint (Franz et al., 2005). This crystalline basement has been suggested to be transgressively overlain by Permo-Triassic siliciclastic Verrucano-type formation sediments followed by dark dolostone and fossiliferous limestones of Upper Triassic to Liassic age and layered cherty limestones of Upper Jurassic to Lower Cretaceous age (Fig. 2) (Dounas et al., 1983; Dürr et al., 1978). The unmetamorphosed Mesozoic sediments may correspond to units of the Lycian Taurus in southwestern Turkey (Katagas and Sapountzis, 1977; Dürr et al., 1978).

New geological map of Kalymnos-Telendos

The major difference between our new geological map of Kalymnos and the IGME 1:50000 map sheet (Dounas et al., 1983) is that two major tectonic contacts, the Telendos Thrust and the Kalymnos Detachment, separate the rocks in three different tectonic units (Fig. 2). Below the Telendos Thrust the newly defined Kefala Unit consists of anchimetamorphic Paleozoic limestones/marbles and dolostones discordantly overlain by a Wildflysch. The Variscan basement, which consists on Kalymnos of amphibolites and garnet bearing quartz micaschists, occurs above the Telendos Thrust and below the Kalymnos Detachment. In analogy with earlier studies (Franz et al., 2005) and correlation with similar rocks in the northern Dodecanese (Roche et al., 2018; 2019) we refer to these amphibolite facies metamorphic rocks as the Marina Basement Unit. The Kalymnos Detachment localized in violet shales at the base of Mesozoic unmetamorphosed limestones, to which we refer as the Marina Cover Unit.

Based on our new geological map of Kalymnos/Telendos and geological field observations (Fig. 2, 3), we discuss in the following these three different units and the tectonic contacts.

Kefala Unit

The Kefala Unit occurs on the small peninsula of Kefala in the north of Kalymnos, at the west coast near Kamari and on the southernmost part of Telendos island (Fig. 2). Internally, the unit consists of refolded anchimetamorphic Paleozoic limestones/marbles and dolostones, which can be separated into lower and upper formations by the Kefala Thrust. The whole package is unconformably overlain by a wildflysch sequence (Fig. 2).The whole unit is exposed in open upright antiforms with km-scale wavelengths possessing subhorizontal NE-SW trending fold axes below the overlying Marina Basement Unit (Fig. 4a-c).

The lower formation of the Kefala Unit consists consist of dark, dm-bedded, partly nodular Upper Paleozoic limestones (KUdbl in Fig. 5) with up to cm-scale crinoid fragments (Fig. 5b), grading into grey, m-scale bedded extremely fossiliferous limestones and dolomites containing bellerophontid, gastropods, brachiopods and orthocone cephalopods (KUd; Fig. 5c). The maximum exposed stratigraphic thickness on Kefala is ~150 m. The nodular limestone layers are interbedded with cm-scale sandy, siliciclastic layers of detrital quartz, muscovite, tourmaline and neoblastic stilpnomelane and actinolite. A pressure solution cleavage wraps around the detrital quartz grains that record no evidence of crystal plastic deformation. In strain shadows of the detrital quartz grains, needles of stilpnomelane and actinolite are present. In the fossiliferous limestones, the lithofacies-types range from densely packed bioclastic packstones, grainstones (Fig. 6a) to micritic-supported wackestones. On the Kefala peninsula the lower formation of the Kefala Unit is deformed into a large type-3 refold structure (Fig. 5a): The first fold has a minimum wavelength of ~150 m and a minimum amplitude of ~50 m with a NNE-SSW trending fold axis and an upright axial plane. The second fold generation has a wavelength of 50 m and an amplitude of 30 m with a NE-SW trending fold axis and a shallow NW-dipping axial plane. In both fold hinges, cm- to dm-spaced stylolites parallel to the axial planes suggest that the deformation mechanism accommodated folding was dissolution-precipitation creep. On Telendos, only the dolostones of the lower formation of the Kefalal Unit, which lacks evidence of folding or refolding, are exposed. The bedding in the dolostones dips generally towards NW to SE (Fig. 2c).

The lower formation is juxtaposed below the upper formation of the Kefala Unit along the Kefala Thrust (Fig. 2b). Both on Telendos and on Kefala peninsula, the thrust zone is characterized by NW-N dipping knife-sharp slickensides, which localized above a m-wide zone of multi-generational dolomitic cataclasites derived from the dolostones of the lower formation (Fig. 5a, d, e). In fact, the intensity of cataclastic deformation increases from the intact dolomites in the footwall towards higher structural levels, from protocataclasites to ultracataclasites at the fault contact of the Kefalal Thrust. The different generations of cataclasites have wavy contacts and injections are locally observed (Fig. 6b).

On the principal slip surfaces, truncated grains are frequently observed. Synthetic Riedel fractures suggest a top-to-SSW/SE transport direction.

The upper formation of the Kefala Unit has an exposed stratigraphic thickness of ~130 m and consists of several white to bright bluish, massive marble sequences with fragments of black crinoids. The rocks are cut by numerous dolomite veins that strike roughly N-S and W-E. At lower structural levels above the Kefala Thrust, several m-wide ductile shear zones transform the otherwise undeformed limestones into dynamically recrystallized fine-grained marble mylonites (Fig. 5f). The N-S striking veins are deformed into ptygmatic folds with fold axes parallel to the shearing direction, recording layer parallel shortening during shearing. Dolomite veins striking W-E are rotated and stretched towards the south into the shearing direction. Stretching is accommodated by boudinage of the dolomite veins, ductile flow in the host calcitic marbles and precipitation of new calcite grains between the interboudin surfaces. Pinch-and-swell shaped objects of dolomite are rotated into the shear direction forming winged inclusions. Note that although at the mesoscopic scale the formation of ptygmatic folds and pinch-and-swell boudinage appear ductile, a closer inspection of the fold hinges and the internal deformation of the winged inclusions reveals the dolomite deforms cataclastically during ductile flow in the host calcitic marbles (Fig. 5f).

At higher structural levels the marbles pass into undeformed limestones and are overlain by several m-thick bedded, fossiliferous, dark limestones with fusulinides (Fig. 5g, 6c, 7a). The limestones are peloid grainstones formed from micritized bioclasts, oncoid rudstones with fragments of skeletal grains forming the centers of biogenous cortices and fusulinid pack- to rudstones (Fig. 6c). The observed lithofacies suggest a shallow water depositional environment on a carbonate shelf under variable energy conditions. Low wave-energy areas are documented by mud- to wackestones containing the stationary semi-infaunal foraminifera globivalvulina. Peloidal grainstones indicate a deposition in a high to moderate energy environment, probably above fair-weather wave base (Flügel, 2010). Originally mineralized organic hard parts (e.g., mollusk and brachiopod shells) were completely fragmented due to reworking by wave or tidal processes in a relatively shallow water environment. Extensive bioerosion by endolithic organisms caused micritic envelops of bioclasts.

Unlike the refold structure in the lower formation of the Kefala Unit, the structures above the Kefala Thrust form an upright low-amplitude dome-and-basin type-1 refold structures with ~100 m wavelength and NNE-SSW and WNW-ESE trending fold axes (Fig. 2b, 4a).

The structures in the lower and upper formations of the Kefala Unit including folding and thrusting indicate a progressive WNW-ESE shortening and are unconformably overlain by a ~80 m-thick wildflysch formation consisting of quartzites, radiolarites, reddish slates, and conglomerates with 10-50 m diameter blocks of marbles and gabbroic rocks embedded in sandstones and conglomerates

without any tectonic contact (7b-d). Here we refer to such sediments composed of a chaotic mass of heterogeneous material of an olistostrome as wildflysch, because this alpine term has been widely used in the regional literature (Papanikolaou and Sideris, 1983). The most spectacular olistoliths are two marble blocks with a ~50 m diameter (Fig. 7b). On Kefala peninsula, the angular unconformity is masked by a WNW-ESE striking brittle fault (Fig. 2). On Telendos, the sedimentary contact of the wildflysch with the underlying unit cross cuts from the upper formation across the Kefala Thrust to the lower formation clearly producing an angular unconformity (Fig. 5d). The whole package was subjected to open upright folding with 10-100 m wavelengths. Deformation in the fold hinges was mainly accommodated by pressure solution and precipitation of arc-normal quartzitic and calcitic composite veins and neither the quartz nor the calcite shows evidence for crystal plastic deformation. Most of the partly chaotic internal deformation probably resulted from soft sediment deformation during mass flow and slumping. In the cm-dm bedded radiolarites and slates, shortened horizons are detached from underlying beds and overlain by undeformed horizontal beds (Fig. 7c). The poorly-sorted matrix-supported conglomerates exhibit reworking of the underlying sediments, and quartzite and radiolarite components occur beside exotic metamorphic and plutonic pebbles (Fig. 7d). The coarse-grained marbles with calcite up to 2 mm record evidence of dynamic recrystallization by grain-boundary migration (black arrow in Fig. 6e). Within the marbles up to several dm-scale angular dolomitic blocks preserve sedimentary structures (Fig. 7b) and undeformed fusulinid foraminifera fossils (white arrow in Fig. 6a) with no indication of metamorphic overprint. Geopedal fabrics are preserved in some of the fossils, which are half filled with micritic sediment and calcite sparite (grey arrow in Fig. 6e).

Telendos Thrust

The Marina Basement Unit is thrusted on top of the Kefala Unit along the newly defined Telendos Thrust. This tectonic contact is exposed around Emborios (Fig. 2 and 5a), west of Kamari and most spectacularly across the southern part of Telendos island (Fig. 2 and 8a). Deformation of the fault rocks along the thrust are dominated by two processes (Fig. 6f-h, 7e and f): (i) Formation of several m-thick multi-generations of cohesive cataclasites to ultracataclasites, some of which could be related to the formation of pseudotachylites. (ii) Dissolution-precipitation processes that overprint rocks from the hanging wall (quartz-mica schists (Fig. 6f, g) and amphibolites (Fig. 6h) of the Marina Basement), footwall (wildflysch of the Kefala Unit, Fig. 7e) and the cataclasites (Fig. 7f) forming SCC' fabrics. Highly deformed shear zones developed in the quartz-rich lithologies by intense formation of pressure solution cleavage parallel to the shear zone boundary (compare Fig. 6f and g). Quartz veins precipitate at high angle to the shear zone boundary and are folded, un-folded and stretched into pinch-and-swells during rotation into the shear direction. Although the deformation of the veins might be accommodated by some contribution of crystal plastic processes, no mylonitic shear zones with a dynamically recrystallized matrix have been observed. All kinematic indicators, such as sigmoids,

SC/SCC' fabric and rotated folded and stretched veins, document a clear top-to-NNW/NNE sense of shear for the Telendos Thrust (Fig. 4e, 6f-h and 7e, f). Shear deformation is strongly localized along the Telendos Thrust with a few isolated shear zones occurring in the hanging wall in the Marina Basement Unit (e.g. Fig. 6h). No structures associated with the Telendos Thrust have been observed in the Kefala Unit.

Marina Basement Unit

The Marina Basement Unit is exposed along the coast northwest of Emborios to Skalia, in Sikati Bay, in the southeast between Masouri and Panormos, in Pithari Bay, and on Telendos (Fig. 2 and 8a). The exposures on Telendos and south of Masouri are dominated >150 m-thick strongly foliated and folded amphibolites (Fig. 7g), which are overlain north of Panormos by ~100 m-thick garnet-bearing quartz mica schists (Fig. 7h). No tectonic contact between the amphibolites and the garnet-bearing quartz mica schists has been observed. The exposures around Emporios and Skalia consist only of quartz mica schists and albite gneisses, where no garnet has been observed. The structures in the Marina Basement Unit are dominated by a complex pattern of refolds, which deform an earlier metamorphic foliation. In general, the foliation is nowhere parallel to the tectonic contacts of the footwall (Telendos Thrust) or hanging wall (Kalymnos Detachment, Fig. 4d). At the outcrop scale the dominant interference patterns are type-3 hook-and-crescent structures best outlined by foliation-parallel quartz veins in the amphibolites (Fig. 7g). Subhorizontal m- to dm-long brittle to brittle/ductile shear zones generally record top-to-N kinematics (Fig. 6h) but brittle top-to-S shear zones have also been locally observed. For a detailed petrological study of the Marina Basement Unit, we refer readers to the work of Franz et al. (2005).

Kalymnos Detachment

The Kalymnos Detachment separates the Marina Basement Unit below from the Marina Cover Unit above (Fig. 8a). Although the contact is largely covered by scree from the cliffs of the Mesozoic limestones, the tectonic contact is well exposed along the roadcuts northwest of Skalia, at the base of the rock-climbing area "The Beach" in Sikati Bay, along the beach in Masouri and at the base of the klippe of Mesozoic limestones on Mt. Vighla (Fig. 2). The several m-thick fault rocks consist mainly of incohesive cataclasites/ultracataclasites and fault gouges, and localize either in phyllonitized crystalline rocks of the Marina Basement Unit or in the Verrucano-type formation violet shales at the base of the Marina Cover Unit (Fig. 8b-d). SC/SCC' fabrics, scaly fabrics and asymmetric boudinage of yellow dolomite layers in the violet shales indicate consistently top-to-SSW shear sense (Fig. 4e). In mature ultracataclasites remnant grains of up to 1 cm in diameter are well rounded and record partly polished clasts surfaces. The fault rocks show highly deformed multi-generations of ultracataclasite formation derived from various strongly altered protoliths with protrusions and injections between the different generations and types of cataclasites (Fig. 8b-d). Brittle to brittle/ductile low-angle shear

zones with top-to-S kinematics with only minor displacement on the order of a few meters to tens of meters are also found in the footwall of the Kalymnos Detachment, for example in the amphibolites and mica schists of the Marina Basement Unit and the wildflysch of the Kefala Unit below the tectonic klippe at Mt. Vighla (Fig. 8e). No low-angle shear zones have been observed in the Marina Cover Unit above the Kalymnos Detachment.

Marina Cover Unit

The Marina Cover Unit consists of violet shales and orange sandstones (Verrucano-type formation) with up to m-thick layers of yellowish dolomites at the base and Mesozoic limestones (Fig. 2), forming up to 350 m high cliffs and representing the dominant lithology of Telendos and Kalymnos (Fig. 2). Although the contact to the underlying basement is clearly tectonic, we use in analogy with previous publications the term 'cover' considering the Marina Cover Unit in a para-autochtonous position. The violet shales are not preserved along the entire base of the Marina Cover Unit and have only been observed in the area of Skalia and Linaria, where they reach a thickness of ~50 m and are tectonically strongly overprinted by the Kalymnos Detachment. The Mesozoic limestones reach a thickness of about 600 m and consist of two parts (Dounas et al., 1983; Tselepidis and Karras, 2013): The lower part includes Late Triassic to Late Jurassic dark, thick bedded limestones with dolomite layers at the base that grades into dark medium to thin-bedded limestones with abundant chert nodules. The upper part is characterized by Cretaceous white-gray, thick-bedded limestones. The contact between the lower and upper carbonate sequence has been described as an angular unconformity (Dounas et al., 1983; Tselepidis and Karras, 2013). Karstification of the limestones resulted in a variety of large- and small-scale features and the development of large cave systems with abundant drip stone formations (e.g., Sikati, Skalia, Fig. 2).

Since the Mesozoic limestones were not the focus of the present study, we refer the reader to more details about the stratigraphy and possible age in the works of Christodoulou (1970), Triantaphyllis and Karfakis (1994), and Tselepides and Karras (2013).

Brittle high-angle fault

All lithologies of the Kefala Unit and the Marina Unit are cut by high-angle WNW-ESE striking brittle normal faults (Fig. 2, 4). These normal faults also control the geomorphology of Kalymnos, characterized by four WNW-ESE striking grabens (Sikati, Arginonta, Vathis and Pothia, Fig. 2) that are filled with Neogene to Quaternary sediments. The high-angle fault, which separates the peninsula of Kefala, is in direct continuation of the Arginonta graben system. In the Kefala Unit, the fault rocks associated with the high-angle normal faults consist of incohesive cataclasites to ultra-cataclasites, where the color can be directly related to the host rocks from which the cataclasites have been derived. Shear sense criteria such as scaly fabrics and synthetic Riedel shears consistently show normal displacement (Fig 8f). Offset of marker horizons at the outcrops south of Masouri and on Telendos

suggest a displacement along these normal faults of only a few meters. Based on the offset of the transgressive contact of the wildflysch on the limestones of the Kefala Unit and the missing continuation of the Telendos Thrust on the Kefala peninsula, the displacement of this normal fault can be estimated on the order of a few tens of meters. Large normal fault scarps are better preserved along the flanks of the graben structures in the Mesozoic limestones of the Marina Unit. Southeast of Arginonta, fault scarps on both sides of the graben are ~50 m high showing corrugated slickensides with a clear dominant dip-slip lineation (Fig. 8g). The partly polished slickensides localized in multi-generational cohesive cataclasites recording truncated grains on the principal slip surface. Synthetic Riedel shears confirm the normal sense of the faults. Locally, the dip-slip lineation is overprinted by a minor dextral strike-slip component (Fig. 4f). In the Skalia cave, WNW-ESE striking normal faults offset and damaged dripstones and flowstones.

Geochronology

We carried out white mica $^{40}Ar/^{39}Ar$ and zircon (U-Th)/He geochronology to resolve the timing of low-temperature deformation of the Kalymnos Detachment and Telendos Thrust (Fig. 9). Multigrain, single crystal total fusion $^{40}Ar/^{39}Ar$ geochronology on handpicked, 106- to 250-µm mica separates from Marina Basement Unit and conglomerates from the Kefala Unit was performed with a Photon Machines CO_2 laser coupled to an ARGUS VI mass spectrometer at the University of Manitoba (Winnipeg, Canada). Additionally, incrementally step-heated $^{40}Ar/^{39}Ar$ geochronology on handpicked mica separates from Marina Basement Unit samples was performed with a Photon Machines CO_2 laser coupled to a Nu Instruments Noblesse multicollector mass spectrometer housed at the Geological Survey of Canada (Ottawa, Canada). Duplicate analyses for four of the five samples was carried out on three- to four-grain aliquots of the 106- to 250-µm size fraction. The methodology and data tables (Table S1 and S2) are available in the supporting information.

Incrementally heated samples are mostly from the Marina Basement Unit exposed north of Emborios; one sample (KA014) was taken from high strain schists of the Telendos Thrust zone. In the mica schists and amphibolites, mica define the planar structure of the rock, occurring as bundles or sheets. All samples monotonically increase in age to an older component preserved in the higher temperature steps (Fig. 10). Total gas ages are ca. 200 Ma to ca. 350 Ma, and notably, the youngest total gas age is from the high strain sample of the Telendos Thrust. Reliable ages are from the older samples defining Carboniferous plateaus, and likely preserve the oldest component recorded in the Marina Basement Unit. Our results are analogous to the muscovite K-Ar dates of Franz et al. (2005), as well as their amphibole K-Ar dates, but the latter set of analyses have extremely low potassium content (~0.5 wt%). Three additional samples within the Telendos Thrust were dated via multiple single crystal $^{40}Ar/^{39}Ar$ analyses, as well as one additional mica schist of Marina Basement Unit. The Marina Basement sample, with white mica defining an anastomosing foliation, yielded a similar dispersion of

dates as the incrementally heated samples, also preserving a middle Carboniferous population as the oldest component. Dates from the thrust zone, comparable to the other latest Triassic date within the high strain zone, are younger. One sample from Telendos island, a deformed calcite-bearing radiolarite, yields a dominant ca. 200 Ma population. The remaining two samples, one west of Kamari and one at Emborios, from the thrust zone yield dominant Late Cretaceous to Paleocene dates from mica that reside in the spaced pressure solution cleavage, which formed during dissolution-precipitation processes.

Following standard mineral separation procedures, individual zircon grains from three samples of the Marina Basement Unit and one sample of the Kefala Unit were handpicked for (U-Th)/He dating. Six to eight zircons from each of the four samples were analyzed at the Thermochronology Research and Instrumentation Laboratory (U-Th)/He facility at the University of Colorado (Boulder, USA). Helium analyses were conducted using an ASI Alphachron He extraction line connected to a Balzers PrismaPlus QME 220 quadrupole mass spectrometer. A Thermo Element 2 magnetic sector mass spectrometer was used for the U and Th analyses. All ages were corrected for the effects of α-ejection and are reported at 2σ analytical uncertainty (Table 1). Details of the (U-Th)/He methodology are available in the supporting information. The new zircon (U-Th)/He data yielded similar dates for all samples, with weighted mean ages of 27.3 ± 0.2 Ma to 30.2 ± 0.4 Ma indicating early Oligocene cooling below ~200°C (Wolfe and Stockli, 2010) for the entire package of crystalline rock on either side of the Telendos Thrust that defines the footwall of the Kalymnos Detachment (Fig. 9). Effective uranium (eU) values range from 939 ppm to 34 ppm, arguably the most retentive zircon analyses with the oldest age at ca. 387 Ma. Notably, the weighted mean (U-Th)/He ages do not include a few single Paleocene dates, which overlap with the youngest single crystal white mica $^{40}Ar/^{39}Ar$ dates (Fig. 10).

Discussion

Tectonic evolution of Kalymnos and correlation of the lithostratigraphy

Based on our new structural observations and geochronological results, we can interpret the tectonic evolution of the units on Kalymnos including the tectonic contacts that separate them. We furthermore discuss our results with previous studies on Kalymnos and attempt to paleogeographically correlate the tectonic units with other studies in the eastern Mediterranean.

Kefala Unit-Kefala Thrust

The rocks of the newly defined Kefala Unit have been previously correlated with the Temenia Unit (Dürr et al., 1978; Katagas, 1980; Franz et al., 2005), the lowermost succession in the Dodecanese, consisting of Paleozoic to Mesozoic sediments overprinted by high-pressure Alpine metamorphism (Franz and Okrusch, 1992). Based on the observation of metamorphic aragonite, blue amphibole, and maximum temperatures determined by Raman spectroscopy on carbonaceous material thermometry, Roche et al. (2018) suggested that the Temenia Unit on Leros experienced Alpine pressures of ~8-10

kbar for temperatures of 370-450°C and, therefore, can be correlated with the Lower Cycladic Blueschist Nappe in the Cyclades (Grasemann et al., 2018). The fossiliferous Upper Paleozoic limestones (Fig. 6a-c) and the quartzites in the discordantly overlying wildflysch (Fig. 6d) show no evidence for extensive dynamic recrystallization and therefore have never experienced temperatures above 300°C (Passchier and Trouw, 2005). Ductile deformation of a limited extent, but still preserving crinoids as clasts and brittle deformation of dolomite veins (Fig. 5f), has been only observed immediately above the brittle fault contact of the Kefala Thrust probably suggesting that this thrust was partly active at the brittle-ductile transition zone with limited dynamic recrystallization in calcite (Bauer et al., 2018). Because the fold-and-thrust belt type deformation of the Upper Paleozoic limestones transgressed by an olistostrome (wildflysch) has not been reported for the Temenia Unit on other islands in the Dodecanese and because the Kefala Unit did not experience high-pressure metamorphism, we suggest that these rocks exposed on the Kefala peninsula of Kalymnos and in the southern parts of Telendos belong to a different tectonic unit (i.e., Kefala Unit), structurally above the Temenia Unit.

The age of the Upper Paleozoic limestones is constrained by the fossil assemblage, especially fusulinids (Fig. 7a), which are shallow warm water benthic foraminifera confined to (sub)tropical conditions. An early Permian age (Asselian-Sakmarian) has been already proposed for the limestones on Kefala by Kahler (1987) and Thorbecke (1987), who emphasized the similarities with faunas in the Carnic Alps, Iran and Central Asia. Although various correlations have been suggested (for a discussion see Robertson and Ustaömer, 2009), very similar lithologies and fauna including fusulinids of late Carboniferous to early Permian age have been reported from the Hadim area in the central Taurides (Kobayashi and Altiner, 2008), Chios (Kahler, 1987), Lesvos (Katsikatsos et al., 1982) and Hydra (Baud et al., 1991, Grant et al., 1991), constraining together with tectonic arguments the paleogeographic position of Kalymnos (see below).

The depositional age of the wildflysch, which unconformably overlies the folded and imbricated Upper Paleozoic limestones, is unknown. The common occurrence of carbonate, chert and large olistoliths signifies intense syntectonic sedimentary activity. The occurrence of a large marble block with dolomite components preserving fusulinid foraminifera (Fig. 6e, 7b) suggests that at least parts of the Paleozoic series experienced low-grade metamorphic conditions, erosion and sedimentation in the wildflysch. Although the style of deformation in the wildflysch unit is completely different and dominated by slumps and soft sediment deformation compared to the underlying folds and faults in the limestones, the rocks below and above the unconformity record both doming and upright, large wavelength folding indicating NW-SE shortening (Fig. 4a-c). On Chios, a pre-Early Triassic wildflysch containing Silurian to Carboniferous olistoliths represents a predominantly Carboniferous accretionary wedge related to the subduction of the Paleotethys (Papanikolaou and Sideris, 1983; Stampfli et al.,

1991; Zanchi et al., 2003), although the details of the stepwise closure of the Paleotethys are more complex (Meinhold et al., 2008; Robertson and Ustaömer, 2009). It is important to emphasize that Christodoulou (1970) reported Upper Carboniferous foraminifera east of Emborios, which he thought were from "limestone lenses" in the Marina Basement Unit. Because the preservation of fossils in marble layers of a highly deformed amphibolite facies rock is very unlikely, we speculate that the reported fossils east of Emborios are from a limestone component within the wildflysch (compare Figs. 6e and 7b). Here, we suggest that the wildflysch on Kalymnos has been deposited in the Triassic on top of the Upper Paleozoic limestones shortly after folding and imbrication along the top-to-SE Kefala Thrust but before being overthrusted by the Marina Unit along the Telendos Thrust (see below). Triassic flysch sedimentation has been reported from several regions in the Alpine-Mediterranean realm and has been attributed to events related to the closure of the Paleotethys (Brandner, 1984) or to rifting of the Neotethys (Robertson et al., 1991). In any case, due to the lack evidence for dynamic recrystallization of quartz, the whole Kefala Unit never experienced anything greater than subgreenschist facies metamorphic conditions. The Oligocene zircon (U-Th)/He age from the wildflysch on Telendos suggests that the Kefala Unit together with the overthrusted Marina Basement Unit experienced its final emplacement at upper crustal levels due to exhumation and cooling below the Kalymnos Detachment.

Marina Basement Unit-Telendos Thrust

The Marina Basement Unit of Kalymnos and Telendos can be related to pre-Alpine basement rocks on the Dodecanese islands of Lipsi, Leros (Katagas and Sapountzis, 1977; Dürr et al., 1978; Katagas, 1980; Franz and Okrusch, 1992; Roche et al., 2018; 2019) and in eastern Crete (Seidel et al., 1982; Franz et al., 2005; Finger et al., 2002; Zulauf et al., 2008). The extent of the Variscan orogen can be traced to the Pelagonian (Kotopouli et al., 2000; Vavassis et al., 2000), the Cyclades (e.g., Andriessen et al., 1987; Tomaschek et al., 2008), and the Sakarya Zone of the Pontides (Meinhold et al., 2008; Okay and Topuz, 2017). Carboniferous tectono-metamorphic processes are interpreted here as the result of northward subduction of the Paleotethys that continued until the Triassic (Brandner, 1984; Stampfli and Borel, 2002), although other paleogeographic reconstructions suggest a subduction of the Paleotethys towards the south (Şengör et al., 1984a; van Hinsbergen et al., 2020).

The Marina Basement Unit in the southern parts of Kalymnos between Masouri and Linari and on Telendos is dominated by amphibolites overlain, without a tectonic contact, by garnet mica schists (Fig. 2). Franz et al. (2005) described these lithologies in the Dodecanese as the Panormos Unit and resolved amphibolite facies conditions of 570-630°C at 5.5-7.5 kbar. Major and trace element geochemistry of amphibolites show striking similarities to Variscan amphibolites in Crete (Franz, 1993). The Marina Basement Unit in the northern parts of Kalymnos between Skalia and the area northwest of Emborios and in Sikati Bay consists only of quartz-rich mica schists and albite gneisses, lacking

garnets. Franz et al. (2005) derived slightly lower metamorphic conditions for these rocks of ~475-550°C and 5.5-6.5 kbar but since the tectonic relation to the metamorphic rocks in the southern part of Kalymnos is not exposed, we refer to all Vasriscan crystalline basement rocks as the Marina Basement Unit. Although these rocks have been compared with similar Variscan-age lithologies on Crete, it is important to emphasized that the Marina Basement Unit not only lacks Alpine high-pressure metamorphism (Franz et al., 2005), but is totally lacking any Alpine metamorphic signature and deformation is only marked by pressure solution cleavage close to the Telendos Thrust. The direct consequence of this observation is that all structures like metamorphic foliation and complex re-folding must be pre-Alpine in age. However, because of the limited exposure and the complexity of the refold structures, we focused on the kinematics of tectonic contacts and did not further investigate the internal pre-Alpine structure of the Marina Basement Unit.

Our proposed tectono-metamorphic history is supported by the published and new geochronological data. Franz et al. (2005) reported K-Ar amphibole ages from the amphibolites in southern Kalymnos (Panormos and Masouri) between 310-230 Ma and K-Ar muscovite ages of 315 Ma from the mica schists northwest of Skalia. Our new $^{40}Ar/^{39}Ar$ ages from the mica schists and amphibolites of the Marina Basement Unit in Kalymnos and Telendos confirm Carboniferous metamorphism but show a clear isotopic resetting of samples in the Triassic at lower structural levels, suggesting a minor thermal event probably related to the closure of the Paleotethys or initial rifting leading to the formation of the Pindos ocean.

The Aegean region during the Late Triassic-Early Jurassic is characterized by deposition of carbonate platforms and pelagic sediments without evidence of orogenesis. Our youngest mica $^{40}Ar/^{39}Ar$ ages from single crystal analysis and in some of the low-temperature steps (Fig. 9 and 10) of material from pressure solution cleavage structures close to the Telendos Thrust yield Cretaceous to Paleocene ages with a dominant group in the Paleocene, which overlaps with the oldest population of zircon (U-Th)/He dates. Since this pressure solution cleavage intensifies in high strain shear zones characterizing the ductile deformation of the Telendos Thrust (compare Fig. 6d, f and g), we suggest that the Telendos Thrust was active in the Paleocene, thrusting the Marina Basement Unit towards the north on top of the Kafala Unit. Note that this tectonic history is significantly different to previous studies, which did not observe a thrust at the base of the Marina Basement Unit, and followed the original idea of Desio (1931) suggesting that the sedimentary rocks of Kalymnos were deposited on a crystalline basement. In this interpretation the Upper Paleozoic limestones exposed on Kefala have a para-autochtonous position and were originally deposited on the Marina Basement Unit (Thorbecke, 1987).

Marina Cover Unit-Kalymnos Detachment

More than 90% of the exposures on the islands of Kalymnos and Telendos consists of the Marina Cover Unit dominated by steep cliffs of the unmetamorphosed Mesozoic limestones. Locally, the base of the limestones is marked by violet shales (Verrucano-type formation), which have been also compared with the Triassic Val Camere Formation of Leros (Desio, 1931; Thorbecke, 1987), the Kapsala Formation of Amorgos (Thorbecke, 1987) and the Tyros Unit in Crete (Zulauf et al., 2018). The violet shales on Kalymnos have been interpreted as a transgressive series, deposited on the eroded Marina Basement Unit (Thorbecke, 1987). Although we do not question the sedimentological interpretation and the stratigraphic position of the protolith of the violet shales, our observations demonstrate that the Kalymnos Detachment localized in this weak lithology and the violet shales have been reworked into fault rocks, which suffered intense polyphase cataclastic deformation at the base of the Marina Cover Unit (Fig. 8c). In fact, the violet shales are tectonically excised and most of the outcrops on Kalymnos and Telendos show that the Mesozoic limestones are directly juxtaposed against the amphibolites and mica schists of the Marina Basement Unit separated by clay gouge and ultracataclasites mainly derived from the crystalline rocks (Fig. 8b, d). The kinematics of the subhorizontal Kalymnos Detachment, which is slightly deformed in three large-wavelength/low-amplitude domes (compare 0 m structure contours of the detachment in Fig. 2), is clearly top-to-SSW and because of the distributed deformation of brittle/ductile shear zones in the footwall of the detachment (Fig. 8e) and an increase in intensity and thickness of cataclastic shear zones towards the base of the Marina Cover Unit, the detachment is interpreted as a low-angle normal fault. Low-angle brittle normal faults with top-to-N kinematics either at the base of the Mesozoic limestones or cutting down-section to deeper structural levels have been reported from Leros, Lipsi and Thymaena and are collectively called here the Thymaena Detachment (Roche et al., 2019). Because our new zircon (U-Th)/He data from the rocks below the Kalymnos Detachment yield Oligocene cooling ages (Fig. 9, Tab. 1), we suggest that the top-to-N extension in the northern Dodecanese and the Kalymnos Detachment were generally simultaneously accommodating bivergent N-S extension of the crust. We emphasize that the Temenia Shear Zone with a top-to-NE kinematics facilitated the syn-orogenic extrusion of the alpine high-pressure/low-temperature rock of the Temenia Unit, which is not exposed on Kalymnos and not related to the post-orogenic Kalymnos Detachment operating at higher structural level.

The Mesozoic limestones of the Marina Cover Unit, which have not been examined stratigraphically in this study, have been discriminated into three different formations (Desio, 1931; Christodoulou, 1970; Dounas et al., 1983; Thorbecke, 1987): (i) The Skalia Limestone has a thickness of about 200 m and consists of dolomites and limestones with stromatolites at the base containing Upper Triassic to Lower Cretaceous microfossils. (ii) The 120 m thick Pantes-Chert-Limestone concordantly overlies the Skalia Limestone and is unconformably overlain by (iii) the 500 m thick Cretaceous

(Hippurites) Elias Limestone. The Mesozoic limestones represents a stratigraphic sequence with no major internal shortening (Thorbecke, 1987) although some imbrications and large-scale folds locally exist (Dounas et al., 1983). Thorbecke (1987) also emphasizes the similarities of the Mesozoic limestones with the units exposed on Amorgos, where the limestones are overlain by Eocene flysch. Eocene limestones and flysch have been also reported from the small island of Pserimos, 5 km east of Kalymnos (Desio, 1931; Christodoulou et al., 1970). Based on these observations plus the important observation that the Marina Cover Unit is in the hanging wall of the Lower Cycladic Blueschist Nappe on Leros, we follow the interpretation of Roche et al. (2018) and suggest that Marina Unit on Kalymnos is similar to the Lycian Nappes of the Pelagonian domain (Roche et al., 2019).

The geomorphology of Kalymnos is dominated by four graben systems, which are associated with normal faults developed in the Mesozoic limestones of the Marina Cover Unit (Fig. 2, 8g) and which are filled with Neogene sediments. Although some local strike-slip reactivation has been observed, the kinematics of the WNW-ESE striking normal faults reflect an overall NNE-SSW extension (Fig. 4f). High-angle faults with the same kinematics have also been observed in the Marina Basement Unit and the Kefala Unit but, with the exception of the fault separating the peninsula of Kefala, these faults record only a few meters of offset. Additionally, neither the Kalymnos Detachment or the Telendos Thrust show significant offset across this graben system and therefore we speculate, that the normal faults, which border the grabens, may root and transfer their displacement into the Kalymnos Detachment. High-angle faults mechanically interacting with low-angle faults have been demonstrated in various detachment systems (e.g., Wernicke, 1981; Lister et al., 1984; Rigo et al., 1996; Gessner et al., 2001; Jolivet et al., 2010) and the orientations of the grabens are aligned with an overall NNE-SSW extension. The strong geomorphological signal of the high-angle normal faults and faulted speleothems in the Skalia cave suggest that these faults are still active accommodating ongoing NNE-SSW extension.

Paleogeographic correlation of the tectonic units on Kalymnos in the eastern Aegean domain

A continuation of the units of Kalymnos and the Dodecanese eastwards to the Lycian Nappes has been already proposed by Bernoulli et al. (1974) and Dürr et al. (1978), although no unequivocal assignment to specific units of the Lycian Nappes has been established. Conversely, Kalymnos rocks have been also assigned either to the Pelagonian (Dürr et al., 1978; Mountrakis, 1986; Schmidt et al., 2020) or the Gavrovo-Tripolitza zone (Papanikolaou and Demirtasli, 1987; Jolivet et al., 2004; Ring et al., 2010). Consequently, no firm correlation with the Hellenides is established either.

Our newly described Kalymnos Detachment juxtaposes Marina Cover carbonates in the hanging wall against Marina Basement and Kefala Unit in the footwall. The Late Triassic-Cretaceous carbonate Marina Cover Unit records locally W-E trending large-scale folds cut by WNW-ESE striking high-angle

brittle normal faults (Triantafyllis and Karfakis, 1994). The Kalymnos Detachment localized at the base of the carbonates along a Verrucano-type formation. A similar lithology can be observed in a comparable structural position in several units throughout the south Aegean such as the Tripolitza Unit of Crete (Stampfli et al., 2003; Zulauf et al., 2008) and the Pelagonian Unit of Attica, Evvia and Hydra (De Bono et al., 2001). The most important stratigraphic feature of Marina Cover is the Cretaceous unconformity (Dounas et al., 1983; Tselepides and Carras, 2013), which is typical for the Pelagonian of continental Greece and related to Vardar ophiolite obduction in the Late Jurassic-Early Cretaceous. Tselepides and Carras (2013) further described continental slope facies that are common for the Pelagonian and non-existant in the Gavrovo-Tripolitza platform. The same unit appears north of Kalymnos on Leros, tectonically overlying the Temenia Unit, a high-pressure metamorphic unit correlative to the CBU (Roche et al., 2018). In Attica and the Cyclades, the CBU is overlain by Pelagonian rocks (Dürr et al., 1978; Papanikolaou, 2009; 2013; Jolivet and Brun, 2010) and there is no simple scenario that could bring the external Gavrovo-Tripolitza rocks on top of the CBU. Therefore, we conclude that the overlying Marina Cover sequence on Kalymnos represents the eastern continuation of the Pelagonian zone.

The underlying Marina Basement of pre-Alpine affinity includes high-grade rocks that were metamorphosed in the Carboniferous (Variscan) and the early Cenozoic (Franz et al., 2005; this study), for instance, during the closure of Pindos basin. Based on lithology, age and metamorphic grade, the Marina Basement bears significant similarities with the Variscan rocks of eastern Crete (Franz et al., 2005; Zulauf et al., 2008). However, the structural position of the two units differs significantly, especially when considering the structure of Leros. On Kalymnos, the Marina Basement tectonically overlies the Kefala Unit, which does not appear either on Leros or eastern Crete. Furthermore, on Leros the Marina Basement overlies the CBU equivalent Temenia Unit. On eastern Crete the Variscan basement is either overlying the more external Phyllite-Quartzite Unit (Stampfli et al., 2003; Zulauf et al., 2008) or the two units are tectonically intercalated (Alexopoulos, 1994). Additionally, Franz et al. (2005) concluded that the Variscan units of Crete have experienced a Miocene high-pressure metamorphic overprint, which is absent in Kalymnos and Leros. Interestingly, analogous lithologies are observed in the Permo-Triassic tectonostratigraphy of the Pelagonian on Evvia, including Verrucano-type Permian-Triassic siliciclastic sediments with Variscan paragneisses and granites as olistholites overlying the Variscan Pelagonian basement (De Bono et al., 2001; Stampfli et al., 2003). This implies that the Carboniferous Marina Basement rocks of Kalymnos and Leros were in a similar position with the Pelagonian basement but followed different paths during the final stages of Paleotethyan closure in the Triassic. Interestingly, some of our new $^{40}Ar/^{39}Ar$ white mica from the Marina Basement rocks record a Triassic signal and may correspond to a thermal pulse related to closure of the Paleotethys or initial rifting leading to the formation of the Pindos ocean.

The Kefala Unit mainly includes Permian shallow water limestones with siliciclastic intercalations unconformably overlain by a wildflysch, most likely Early Triassic in age (Kahler, 1987; this study). Permian limestones are generally rare in the Hellenides, but are found throughout the Pelagonian, for example in Chios, Lesvos, Hydra, Salamis, Attica, and Evvia (Thorbecke, 1987; Grant et al., 1991) but occur also as blocks within late Permian-Triassic clastic sequences (Baud et al., 1991; De Bono et al., 2001; Stampfli et al., 2003). The Permian limestones of Kalymnos show marked similarities with those described on the Pelagonian Hydra Island, west of the Cyclades, and the uncomformably overlying wildflysch resembles the Permian-Triassic clastic sequences including blocks of Permian carbonates, metacherts and metabasites (Grant et al., 1991).

Although the oldest stratigraphic age of the Kefala Unit is unknown, at least the exposed Permian part is too young to be affected by the Variscan event, which is responsible for Carboniferous granitic intrusions found in the Pelagonian and Cycladic basement. Nevertheless, the limestones of the Kefala Unit record a complex tectonic history including folding, re-folding and the top-to-S stacking along the brittle/ductile Kefala Thrust, which is sealed by the wildflysch. Since such an event is only reported in this study from Kalymnos, it probably represents localized upper crustal shortening, which may be associated with the Triassic closure of the Paleotethys. The Kefala Unit is overthrusted by the Marina Basement Unit along the top-to-N Telendos Thrust. Contrary to Kefala Thrust, the Telendos Thrust is a large-scale brittle-ductile fault, observed over a thrust-length of at least 20 km. Multiple single grain white mica $^{40}Ar/^{39}Ar$ dating from spaced foliation close to the Telendos Thrust and mylonitic foliation formed by dissolution-precipitation creep from the Telendos Thrust yielded a cluster of Paleocene ages. Temporally, this coincides with the onset of the Cenozoic closure of the Pindos, which is generally associated with a top-to-SW kinematics (Jolivet and Brun, 2010; Ring et al., 2010; Papanikolaou, 2013, Zulauf et al., 2019). Interestingly, within the Pelagonian, folds and thrusts are reported from the peninsula of Argolis (Bortolotti et al., 2003), from the island Amorgos (Chatzaras et al., 2011) and from Santorini, where Eocene flysch is folded in a NW-vergent synclline (Schneider et al., 2018). Our structural and geochronological data indicate that the Telendos Thrust is another structure that is associated with an early episode of top-to-N back-thrusting within the orogenic wedge above the north-dipping subduction zone. Within this retro-wedge the Variscan Marina Basement Unit was translated onto the more internal Kefala Unit prior to the 50-52 Ma peak HP metamorphism of the CBU (Lagos et al., 2007). Interestingly, a retro-extrusion has been also suggested for the Eocene/Oligocene exhumation of high-pressure unit of the CBU (e.g. Xypolias et al., 2012; Gerogiannis and Xypolias, 2017).

All these observations suggest that the Kefala Unit and the other units on Kalymnos are located in a northern position than the Paleotethyan suture and the Pindos-CBU domain at the southern margin of the Pelagonian domain. Putting all of these observations together, we propose the following

692 model for the late Paleozoic to Cenozoic paleogeographic evolution of Kalymnos and homologous units
693 in the Aegean:

694 In the late Permian (Fig. 11a) north to northwest subduction of Paleotethys has already shaped
695 the Pelagonian basement, which extends from northwestern continental Greece to the southeast
696 Aegean, including areas such as Chios, Evvia, Attica, Argolis, Hydra and Kalymnos. The Variscan
697 basement is locally exposed and eroded in small rifts thus Verrucano-type siliciclastic deposits are
698 produced (Baud et al., 1991; De Bono et al., 2001; Stampfli et al., 2003). In some places like Evvia,
699 Hydra and Kalymnos, Permian reefs are developed with minor or more significant intervals of
700 siliciclastic material. Rifting of the northern part of Gondwana resulted in opening of the Neotethys
701 ocean.

702 In the Early Triassic (Fig. 11b), the Paleotethyan closure resulted in initial collision and deposition
703 of the Variscan basement and Permian rocks are recorded in olistostromes (e.g. in eastern Crete) and
704 in the outer Paleotethyan arc (Phyllite-Quartzite Unit, Tyros/Ravdoucha beds). On Kalymnos in the
705 Kefala Unit, limestones are folded and internally imbricated along the Kefala Thrust. This process may
706 have locally started earlier as indicated by late Permian meta-volcanoclastic sequences derived from
707 the Variscan Cycladic Basement on Ios and Sikinos islands (Poulaki et al., 2019).

708 Subsequent Middle Triassic rifting and formation of the Pindos-CBU domain has dissected the
709 Paleotethyan accretionary prism and Variscan basement (Fig. 11c). The northern segment includes the
710 Mesozoic sequences of the Pelagonian domain whereas the southern segment comprises the
711 Tyros/Ravdoucha beds at the base of the Tripolitza-Gavrovo platform and the Phyllite-Quartzite Unit.
712 Volcanic activity is widespread, producing Anisian-Carnian volcanoclastic sequences found throughout
713 the Aegean domain (Pe-Piper and Piper, 2002). On Kalymnos, parts of the Marina Basement Unit are
714 exhumed to the upper crust and the Verrucano-type formation is deposited atop the Kefala Unit and
715 exposed Variscan basement.

716 The Late Triassic is tectonically quiescent. The Neotethys, Pindos-CBU and Vardar-Axios oceanic
717 domains continue to grow and carbonate platforms are deposited above the volcanoclastic sequences
718 of the External Hellenides and the Pelagonian domain (Fig. 11d).

719 In the Paleocene-Eocene (Fig. 11e), the subduction of the Pindos-CBU domain beneath the
720 Pelagonian upper plate has produced the Late Cretaceous magmatic arc (Martha et al., 2017;
721 Koutsovitis et al., 2021). The CBU is subducted to blueschist- and eclogite-facies high-pressure
722 metamorphic condition (Jolivet and Brun, 2010; Ring et al., 2010). Shortening of the upper plate
723 resulted in local back-thrusts and the top-to-N Telendos Thrust has brought Marina Basement Unit
724 above the Kefala Unit in a retro-wedge setting. The overlying Mesozoic sequences are folded with

N/NW-verging folds, antithetic to the general kinematics of the nappe stacking followed by extrusion in the subduction channel (Grasemann et al, 2018).

Cenozoic tectonic evolution at the Aegean-Anatolian transition zone

West of the Menderes Massif and east of Cyclades, the Dodecanese islands formed in the same tectonic setting with a very similar evolution, commencing with Cretaceous subduction underneath the southern margin of Eurasia, Late Cretaceous obduction of the Vardar oceanic crust, Paleocene-Eocene subduction of the Pindos basin and the northern margin of Pindos with formation and exhumation of the Lower Cycladic Blueschist Nappe (i.e., Temenia unit), transitioning to post-orogenic extension in the back-arc region during the Oligocene and Miocene (e.g., Jolivet and Brun, 2010; Ring et al, 2010; Grasemann et al., 2012; Papanikolaou, 2013; Roche et al., 2019).

The western and central Cyclades record bivergent extension along the top-to-N to -NE North Cycladic Detachment System and Naxos Paros Detachment System with respect to the top-to-S to -SW West Cycladic Detachment System, Santorini Detachment System and a debated South Cycladic Detachment System (Lister et al., 1984; Gautier et al., 1993; Jolivet et al, 2010; Ring et al., 2011; Grasemann et al., 2012; Schneider et al., 2018). In western Anatolia, the Menderes Metamorphic Core Complex has been also exhumed along the bivergent Büyük Menderes and the Gediz detachments (Hetzel et al, 1995; Gessner et al., 2001), preceded by the top-to-N Simav Detachment starting in the Oligocene. Similar to the western and central Cyclades, extension continued into the middle-late Miocene (Ring et al., 2003; Bozkurt et al., 2011). It has been suggested that the differential deformation between the low-angle detachment systems in the Cyclades and the Menderes Metamorphic Core complex has been accommodated by a N-S to NNE-SSW striking lithospheric-scale sinistral wrench corridor probably related slab break off or tearing at the leading edge of the Anatolide-Tauride continent (Ring et al., 1999a; Sözbilir et al., 2011; Gessner et al., 2013; Jolivet et al., 2015; Uzel et al., 2015; Ring et al., 2017). Although, some of these accommodation zones like the İzmir-Balıkesir Transfer Zone (Uzel et al., 2015) are more restricted to the northwestern part of Anatolia, other studies suggest a transtensional West Anatolia Transfer Zone forming a corridor of heterogeneously distributed extension from northwestern Anatolia in the north to the Dodecanese islands in the south (Gessner et al., 2013; Jolivet et al., 2015; Ring et al., 2017). However, Roche et al. (2019) demonstrated that that the direction of extension in the northern Dodecanese is consistently top-to-NNE related to low-angle normal faults of the Thymaena Detachments without any evidence for strike-slip fault systems, which are expected above a slab tear. This observation suggests that a non-localized, relatively wide zone of distributed brittle/ductile deformation in the upper crust accommodated the left-lateral displacement imposed by the faster retreat of the slab south of the Aegean domain compared to the retreat south of Anatolia (Roche et al., 2019) and the induced flow in the asthenospheric mantle is accommodated by top-to-N low-angle shear zones in the crust (Jolivet et al., 2015; Menant et al., 2016).

In contrast to the top-to-N Thymaena Detachments (Roche et al., 2019), our work shows that Kalymnos and Telendos in the central Dodecanese was subjected to top-to-SSW extension along the Kalymnos Detachment (Fig. 12). Thus, comparable to the Cyclades and Menderes Massif, the Aegean-Anatolian transition zone is also characterized by bivergent extension. Similar to the northern Dodecanes (Roche et al., 2018; 2019), we did not find evidence of strike-slip deformation. Our new zircon (U-Th)/He ages indicate that extension started in the Oligocene but detachment-related high-angle faults with Neogene sediments in the graben suggest ongoing extension with similar kinematics into the Miocene. It is tempting to correlate the Kalymnos Detachment with the Neogene brittle detachment fault described on Kos island, 10 km south of Kalymnos (van Hinsbergen and Boekhout, 2009). On Kos, Permo-Carboniferous rocks, intruded and locally metamorphosed by a 12 Ma old monzonite intrusion (Altherr et al., 1976), are juxtaposed against Upper Mesozoic non-metamorphosed carbonate units along a top-to-N low-angle fault (van Hinsbergen and Boekhout, 2009). Because of the geological similarities with the Kalymnos Detachment, we suggest two scenarios, which are subject to further investigations: (i) The detachment on Kos is an isolated structure with opposing kinematics to the Kalymnos Detachment. (ii) The top-to-N shear sense described in van Hinsbergen and Boekhout (2009) is related to high-angle structures (46-60° dips in figure 4 of van Hinsbergen and Boekhout, 2009). These structures could be antithetic high-angle bookshelf faults related to a top-to-S detachment (Mandl, 1987) representing a possible southern continuation of the Kalymnos Detachment.

Compared to the bivergent extension in the Menderes Massif and the Cyclades, the bivergent extension in the Dodecanese islands is restricted to shear localization in the mainly brittle to brittle/ductile upper crust showing almost no greenschist facies overprint of the syn-orogenic high-pressure rocks in the Temenia Unit in the northern Dodecanese (Roche et al., 2018). Similarly, the Paleocene Telendos Thrust and Oligo-Miocene Kalymnos Detachment operated mainly in the upper crust and therefore the Marina Basement Unit and the Kefala Unit escaped significant Alpine metamorphic overprint. It is appealing to relate the shallow crustal low-angle extension in the Dodecanes, compared to the much stronger post-orogenic deformation and metamorphic overprint in the Cyclades, with the transitional position above the slab tearing at the leading edge of the Anatolide-Tauride continent. We suggest that the onset of extension in the Dodecanese at 35-30 Ma resulted mainly from the rollback of the slab, which is more important in the Aegean Sea than in western Turkey. Before the onset of post-orogenic extension, southward propagation of syn-orogenic thrusting continued at the proximal margin of the Pindos ocean with understacking of the Temenia Unit (Lower Cycladic Blueschist Unit) below Marina Basement and Cover Unit (i.e., Lycian Nappes). Rapid exhumation of the Temenia Unit below the top-to-N syn-orogenic Temenia Shear Zone facilitated the preservation of high-pressure/low-temperature parageneses (Roche et al., 2019). Post-orogenic

extension started in the upper structural level of the brittle crust with low-angle normal faults along the Kalymnos Detachment (top-to-S) and the Thymaena Detachment (top-to-N). The timing of slab tearing below the Aegean-Anatolian transition zone is still debated and tearing of the slab has been suggested to start in the Campanian (Okay et al., 1998; Okay and Whitney, 2010), in the early Eocene (e.g., Karacik et al., 2008; Dilek and Altunkaynak, 2009; Ustaömer et al., 2009; Altunkaynak et al., 2012; Ersoy and Palmer, 2013), in the Oligocene (Govers and Fichtner, 2016) or in the middle Miocene (e.g., Faccenna et al., 2003; van Hinsbergen et al., 2010; Erkül and Erkül, 2012; Jolivet et al., 2013; Pourteau et al., 2013). Our new data support a consistent bivergent N-S extension in the Aegean-western Anatolian region starting in the Oligocene and suggest that this extension initiated before the slab tearing affected differential extension in the Cyclades and the Menderes Massif. Low-angle extension in the Dodecanes continued in the Miocene mechanically interacting with high-angle faults, which controlled sediment deposition in WNW-ESE trending grabens with no evidence of a significant strike slip component.

Conclusions

1) The tectonic position above the Lower Cycladic Blueschist Nappe and correlation with other units in the Aegean suggest that the Central Dodecanese (Kalymnos/Telendos) at the Aegean-Anatolian transition zone is not part of the External Hellenides, but was paleogeographically located at the southern margin of Pelagonia.

2) Alpine deformation on Kalymnos was restricted to the upper crust and therefore a Variscan basement, a Permo-Triassic fold-and-thrust belt sealed by wildflysch and a weak Triassic thermal event have been preserved.

3) In the Paleocene during the onset of closure of the Pindos, the central Dodecanese were in the position of a retro-wedge and the southern margin of the Pelagonian was subjected to shortening and top-to-N thrusting along the Telendos Thrust. The Telendos Thrust is a major structure, which thrusted a slice of the Variscan basement with the Mesozoic cover to the north and can be traced over a thrust length of more than 20 km.

4) Oligo-Miocene extension was accommodated along the top-S Kalymnos Detachment, localizing between the Variscan basement and the unmetamorphosed Mesozoic limestones in Verrucano-type sediments. Coeval top-to-N extension in the northern Dodecanese suggests that the Aegean-Anatolian transition zone was, similar to the Cyclades and the Menderes Massif, subjected to bivergent extension.

5) WNW-ESE striking high-angle faults control the geomorphology of Kalymnos, characterized by four WNW-ESE striking grabens that are filled with Neogene to Quaternary sediments. Some of these faults may be still active causing damage of speleothems in the caves of Kalymnos. This observation suggests that the central Dodecanese at the Aegean-Anatholian transition were subjected to N-S extension since the Oligocene with no evidence for a major strike-slip corridor accommodating differential extensional strain between Menderes and Attic-Cycladic core complexes.

Acknowledgement

Funding was provided by the Austrian Academy of Sciences (Emil Suess-Erbschaft) and by the Natural Sciences and Engineering Research Council of Canada. We thank the Greek Institute for Mining and Exploration (IGME) in Athens for providing permission of fieldwork and technical support. Laboratory assistance from Jim Metcalf (University of Colorado), Alfredo Camacho (University of Manitoba), and Nancy Joyce (Geological Survey of Canada) is greatly appreciated. We acknowledge fruitful discussions with A. Rogowitz, A.H.N. Rice, B. Huet, L. Plan and E. Chatziioannou.

References

Aktug, B., Nocquet, J. M., Cingöz, A., Parsons, B., Erkan, Y., England, P., Lenk, O., Gürdal, M. A., Kilicoglu, A., Akdeniz, H., and Tekgül, A., 2009, Deformation of western Turkey from a combination of permanent and campaign GPS data: Limits to block-like behavior: Journal of Geophysical Research: Solid Earth, v. 114, no. B10.

Alexopoulos, A., 1994, Variscan metamorphic rocks of central-east Crete and their significance for the geotectonic position of the Phyllite-Quartzite Unit: Bulletin of the Geological Society of Greece, v. XXX, no. 2, p. 153-158.

Altherr, R., Keller, J., and Kott, K., 1976, Der jungtertiäre Monzonit von Kos und sein Kontaktof (Agäis, Griechenland): Bulletin de la Société Géologique de France v. 7, p. 403-412.

Altunkaynak, Ş., Sunal, G., Aldanmaz, E., Genç, C. Ş., Dilek, Y., Furnes, H., Foland, K. A., Yang, J., and Yıldız, M., 2012, Eocene Granitic Magmatism in NW Anatolia (Turkey) revisited: New implications from comparative zircon SHRIMP U-Pb and ^{40}Ar-^{39}Ar geochronology and isotope geochemistry on magma genesis and emplacement: Lithos, v. 155, p. 289-309.

Andriessen, P. A. M., Banga, G., and Hebeda, E. H., 1987, Isotopic age study of pre-Alpine rocks in the basal units on Naxos, Sikinos and Ios, Greek Cyclades: Geologie en Mijnbouw, v. 66, p. 3-14.

859 Aubouin, J., and Dercourt, J., 1970, Sur la geologie de l'Egee; regard sur le Dodecanese meridional
860 (Kasos; Karpathos; Rhodes): Bulletin de la Société Géologique de France, v. S7-XII, no. 3, p. 455-
861 472.

862 Baldwin, S. L., and Lister, G. S., 1998, Thermochronology of the South Cyclades Shear Zone, Ios, Greece:
863 Effects of ductile shear in the argon partial retention zone: Journal of Geophysical Research, v.
864 103, no. B4, p. 7315-7336.

865 Baud, A., Jenny, C., Papanikolaou, D., Sideris, C., and Stampfli, G. M., 1991, New observations on
866 Permian stratigraphy in Greece and geodynamic implication: Bulletin of the Geological Society
867 of Greece, v. 25, p. 187-206.

868 Bauer, H., Rogowitz, A., Grasemann, B., and Decker, K., 2018, Intracrystalline deformation of calcite in
869 the upper brittle crust: Geology, v. 46, no. 4, p. 375-378.

870 Berk Biryol, C., Beck, S. L., Zandt, G., and Özacar, A. A., 2011, Segmented African lithosphere beneath
871 the Anatolian region inferred from teleseismic P-wave tomography: Geophysical Journal
872 International, v. 184, no. 3, p. 1037-1057.

873 Bernoulli, D., Graciansky, P. C., and Monod, O., 1974, The extension of the Lycian Nappes (SW Turkey)
874 into the southeastern Aegean Islands: Eclogae Geologicae Helvetiae, v. 67, p. 39-90.

875 Blake Jr., M. C., Bonneau, M., Geyssant, J., Kienast, J. R., Lepvrier, C., Maluski, H., and Papanikolaou,
876 D., 1981, A geological reconnaissance of the Cycladic blueschist belt, Greece: Geological Society
877 of America Bulletin, v. 92, p. 247-254.

878 Bonneau, M., 1984, Correlation of the Hellenide nappes in the south-east Aegean and their tectonic
879 reconstruction, in Dixon, J. E., and Robertson, A. H. F., eds., The Geological Evolution of the
880 Eastern Mediterranean, Volume 17: London, Geological Society, London, Special Publications, p.
881 517-527.

882 Bortolotti, V., Carras, N., Chiari, M., Fazzuoli, M., Marcucci, M., Photiades, A., and Principi, G., 2003,
883 The Argolis peninsula in the palaeogeographic and geodynamic frame of the Hellenides: Ofioliti,
884 v. 28, no. 2, p. 79-94.

885 Bozkurt, E., and Oberhänsli, R., 2001, Menderes Massif (Western Turkey): structural, metamorphic and
886 magmatic evolution - a synthesis: International Journal of Earth Sciences, v. 89, no. 4, p. 679-
887 708.

888 Bozkurt, E., Satır, M., and Buğdaycıoğlu, Ç., 2011, Surprisingly young Rb/Sr ages from the Simav
889 extensional detachment fault zone, northern Menderes Massif, Turkey: Journal of Geodynamics,
890 v. 52, no. 5, p. 406-431.

891 Brandner, R., 1984, Meeresspiegelschwankungen und Tektonik in der Trias der NW-Tethys.: Jahrbuch
892 der Geologischen Bundesanstalt (Wien), v. 126, no. 4, p. 435-475.

893 Brun, J.-P., and Faccenna, C., 2008, Exhumation of high-pressure rocks driven by slab rollback: Earth
894 and Planetary Science Letters, v. 272, no. 1-2, p. 1-7.

895 Candan, O., Dora, O. Ö., Oberhänsli, R., Oelsner, F., and Dürr, S., 1997, Blueschist relics in the Mesozoic
896 cover series of the Menderes Massif and correlations with Samos Island, Cyclades:
897 Schweizerische Mineralogische and Petrographische Mitteilungen, v. 77, p. 95-99.

898 Candan, O., Cetinkaplan, M., Oberhansli, R., Rimmelé, G., and Akal, C., 2005, Alpine high-P/low-T
899 metamorphism of the Afyon Zone and implications for the metamorphic evolution of Western
900 Anatolia, Turkey: Lithos, v. 84, no. 1-2, p. 102-124.

901 Çetinkaplan, M., Candan, O., Oberhänsli, R., Sudo, M., and Cenki-Tok, B., 2020, P–T–t evolution of the
902 Cycladic Blueschist Unit in Western Anatolia/Turkey: Geodynamic implications for the Aegean
903 region: Journal of Metamorphic Geology, v. 38, no.4, p. 379-419.

904 Chatzaras, V., Xypolias, P., Kokkalas, S., and Koukouvelas, I., 2011, Oligocene-Miocene thrusting in
905 central Aegean: insights from the Cycladic island of Amorgos: Geological Journal, v. 46, no. 6, p.
906 619-636.

907 Christodoulou, G., 1970, Some remarks on the geology of Kalymnos island (Dodecane) and the age of
908 its formations: Annales Geologique de Pays Hellenique, v. 21, p. 307-319.

909 Collins, A. S., and Robertson, A. H. F., 1997, Lycian melange, southwestern Turkey: An emplaced Late
910 Cretaceous accretionary complex: Geology, v. 25, no. 3, p. 255-258.

911 Cordey, F., and Quillévéré, F., 2019, Reassessing the age of Karpathos ophiolite (Dodecanese, Greece):
912 consequences for Aegean correlations and Neotethys evolution: Geological Magazine, v. 157,
913 no. 2, p. 263-274.

914 Creutzburg, N., and Seidel, E., 1975, Zum Stand der Geologie des Präneogens auf Kreta: Neues Jahrbuch
915 für Geologie und Paläontologie Abhandlungen, v. 149, p. 363-383.

916 Creutzburg, N., Drooger, C. W., Meulenkamp, J. W., Papastamatiou, J., Seidel, E., and Tataris, A., 1977,
917 General Geological Map of Crete: Institute of Geological and Mining Exploration (IGME), scale
918 1:200,000.

De Bono, A., Martini, R., and Zaninetti, L., 2001, Permo-Triassic stratigraphy of the pelagonian zone in central Evia island (Greece): Eclogae Geologicae Helvetiae = Swiss journal of geosciences, v. 94, no. 3, p. 289-311.

Desio, A., 1931, Le isole italiane dell'Egeo, Roma, Memorie descrittive della carta geologica d'Italia, 534 p.

Dilek, Y., and Altunkaynak, Ş., 2009, Geochemical and temporal evolution of Cenozoic magmatism in western Turkey: mantle response to collision, slab break-off, and lithospheric tearing in an orogenic belt: Geological Society, London, Special Publications, v. 311, no. 1, p. 213-233.

Dounas, A. G., Kakavas, N. J., and Tassios, N. P., 1983, Geological map of Greece, sheet Kalymnos island Athens.: IGME, scale 1: 50000.

Dürr, S., Altherr, R., Keller, J., Okrusch, M., and Seidel, E., 1978, The median Aegean crystalline belt: stratigraphy, structure, metamorphism, magmatism, in Cloos, H., Roeder, D., and Schmidt, K., eds., Alps, Apennines, Hellenides, Volume 38: Stuttgart, Schweizerbart, p. 455-476.

Dürr, S., 1986, Die Karischen Inseln zwischen Samos und Karpathos-Rhodos, in Jacobshagen, V., ed., Geologie von Griechenland: Berlin, Borntraeger, p. 180-187.

Erkül, S. T., and Erkül, F., 2012, Magma interaction processes in syn-extensional granitoids: The Tertiary Menderes Metamorphic Core Complex, western Turkey: Lithos, v. 142-143, p. 16-33.

Ersoy, E. Y., and Palmer, M. R., 2013, Eocene-Quaternary magmatic activity in the Aegean: Implications for mantle metasomatism and magma genesis in an evolving orogeny: Lithos, v. 180-181, p. 5-24.

Faccenna, C., Jolivet, L., Piromallo, C., and Morelli, A., 2003, Subduction and the depth of convection in the Mediterranean mantle: Journal of Geophysical Research: Solid Earth, v. 108, no. B2 2099, doi:10.1029/2001JB001690

Fassoulas, C., Kilias, A., and Mountrakis, D., 1994, Postnappe stacking extension and exhumation of high-pressure/low-temperature rocks in the island of Crete, Greece: Tectonics, v. 13, no. 1, p. 127-138.

Finger, F., Krenn, E., Riegler, G., Romano, S., and Zulauf, G., 2002, Resolving Cambrian, Carboniferous, Permian and Alpine monazite generations in the polymetamorphic basement of eastern Crete (Greece) by means of the electron microprobe: Terra Nova, v. 14, no. 4, p. 233-240.

Flügel, E., 2010, Microfacies of Carbonate Rocks: Analysis, Interpretation and Application Berlin, Springer, 984 p.

Forster, M. A., and Lister, G. S., 1999, Detachment faults in the Aegean core complex of Ios, Cyclades, Greece, in Ring, U., Brandon, M. T., Lister, G. S., and Willet, S. D., eds., Exhumation Processes: Normal Faulting, Ductile Flow and Erosion, Volume 154, The Geological Society of London, p. 305-323.

Franz, L., and Okrusch, M., 1992, Aragonite-bearing blueschists on Arki Island, Dodecanese, Greece: European Journal of Mineralogy, v. 4, no. 3, p. 527-537.

Franz, L., 1993, Geochemische Untersuchungen von präalpidischen Amphiboliten der Insel Kreta und des Dodekanes (Griechenland): Zeitschrift der Deutschen Geologischen Gesellschaft, v. 144, p. 121-127.

Franz, L., Okrusch, M., Seidel, E., and Kreuzer, H., 2005, Polymetamorphic evolution of pre-Alpidic basement relics in the external Hellenides, Greece: Neues Jahrbuch für Mineralogie, Abhandlungen, v. 181, no. 2, p. 147-172.

Gautier, P., Brun, J.-P., and Jolivet, L., 1993, Structure and kinematics of Upper Cenozoic extensional detachment on Naxos and Paros (Cyclades Islands, Greece): Tectonics, v. 12, no. 5, p. 1180-1194.

Gerogiannis, N., and Xypolias, P., 2017, Retroward extrusion of high-pressure rocks: An example from the Hellenides (Pelion Blueschist Nappe, NW Aegean): Terra Nova, v. 29, no. 6, p. 372-381.

Gessner, K., Ring, U., Johnson, C., Hetzel, R., Passchier, C. W., and Güngör, T., 2001, An active bivergent rolling-hinge detachment system: Central Menderes metamorphic core complex in western Turkey: Geology, v. 29, no. 7, p. 611-614.

Gessner, K., Gallardo, L. A., Markwitz, V., Ring, U., and Thomson, S. N., 2013, What caused the denudation of the Menderes Massif: Review of crustal evolution, lithosphere structure, and dynamic topography in southwest Turkey: Gondwana Research, v. 24, no. 1, p. 243-274.

Göncüoğlu, M. C., Dirik, K., and Kozlu, H., 1997, General characteristics of pre-Alpine and Alpine Terranes in Turkey: Explanatory notes to the terrane map of Turkey: Annales Geologique de Pays Hellenique, v. 37, p. 515-536.

Govers, R., and Fichtner, A., 2016, Signature of slab fragmentation beneath Anatolia from full-waveform tomography: Earth and Planetary Science Letters, v. 450, p. 10-19.

Grant, R. E., Nestell, M. K., Baud, A., and Jenny, C., 1991, Permian Stratigraphy of Hydra Island, Greece: Palaios, v. 6, no. 5, p. 479-497.

979 Grasemann, B., Schneider, D. A., Stöckli, D. F., and Iglseder, C., 2012, Miocene bivergent crustal
980 extension in the Aegean: Evidence from the western Cyclades (Greece): Lithosphere, v. 4, no. 1,
981 p. 23-39.

982 Grasemann, B., Huet, B., Schneider, D. A., Rice, A. H. N., Lemonnier, N., and Tschegg, C., 2018, Miocene
983 postorogenic extension of the Eocene synorogenic imbricated Hellenic subduction channel: New
984 constraints from Milos (Cyclades, Greece): GSA Bulletin, v. 130, no. 1-2, p. 238-262.

985 Grasemann, B., Schneider, D. A., and Rogowitz, A., 2019, Back to normal: Direct evidence of the Cretan
986 Detachment as a north-directed normal fault during the Miocene: Tectonics, v. 38, no. 8, p.
987 3052-3069.

988 Heineke, C., Hetzel, R., Nilius, N.-P., Zwingmann, H., Todd, A., Mulch, A., Wölfler, A., Glotzbach, C., Akal,
989 C., Dunkl, I., Raven, M., and Hampel, A., 2019, Detachment faulting in a bivergent core complex
990 constrained by fault gouge dating and low-temperature thermochronology: Journal of Structural
991 Geology, v. 127, p. 103865.

992 Hetzel, R., Passchier, C. W., Ring, U., and Dora, O. O., 1995, Bivergent extension in orogenic belts: The
993 Menderes Massif (southwestern Turkey): Geology, v. 23, p. 455-458.

994 Huet, B., Labrousse, L., and Jolivet, L., 2009, Thrust or detachment? Exhumation processes in the
995 Aegean: Insight from a field study on Ios (Cyclades, Greece): Tectonics, v. 28, no. 3, p. TC3007.

996 Jacobshagen, V., Dürr, S., Kockel, F., Kopp, K. O., and Kowalczky, G., 1978, Structure and Geodynamic
997 Evolution of the Aegean region, in Cloos , H., Roeder, D., and Schmidt, K., eds., Alps, Apennines,
998 Hellenides: Stuttgart, Schweizerbart, p. 537-564.

999 Jolivet, L., Goffé, B., Monié, P., Truffert-Luxey, C., Patriat, M., and Bonneau, M., 1996, Miocene
1000 detachment in Crete and exhumation P-T-t paths of high-pressure metamorphic rocks:
1001 Tectonics, v. 15, no. 6, p. 1129-1153.

1002 Jolivet, L., Faccenna, C., Goffe´, B., Burov, E., and Agard, P., 2003, Subduction tectonics and exhumation
1003 of high-pressure metamorphic rocks in the Mediterranean orogens: American Journal of
1004 Science, v. 3003, no. 4, p. 353-409.

1005 Jolivet, L., Rimmelé, G., Oberhansli, R., Goffe, B., and Candan, O., 2004, Correlation of syn-orogenic
1006 tectonic and metamorphic events in the Cyclades, the Lycian nappes and the Menderes massif.
1007 Geodynamic implications: Bulletin de la Societe Geologique de France, v. 175, no. 3, p. 217-238.

1008 Jolivet, L., and Brun, J.-P., 2010, Cenozoic geodynamic evolution of the Aegean: International Journal
1009 of Earth Sciences, v. 99, no. 1, p. 109-138.

1010 Jolivet, L., Lecomte, E., Huet, B., Denèle, Y., Lacombe, O., Labrousse, L., Le Pourhiet, L., and Mehl, C.,
1011 2010, The North Cycladic Detachment System: Earth and Planetary Science Letters, v. 289, no.
1012 1-2, p. 87-104.

1013 Jolivet, L., Faccenna, C., Huet, B., Labrousse, L., Le Pourhiet, L., Lacombe, O., Lecomte, E., Burov, E.,
1014 Denèle, Y., Brun, J.-P., Philippon, M., Paul, A., Salaün, G., Karabulut, H., Piromallo, C., Monié, P.,
1015 Gueydan, F., Okay, A. I., Oberhänsli, R., Pourteau, A., Augier, R., Gadenne, L., and Driussi, O.,
1016 2013, Aegean tectonics: Strain localisation, slab tearing and trench retreat: Tectonophysics, v.
1017 597-598, p. 1-33.

1018 Jolivet, L., Menant, A., Sternai, P., Rabillard, A., Arbaret, L., Augier, R., Laurent, V., Beaudoin, A.,
1019 Grasemann, B., Huet, B., Labrousse, L., and Le Pourhiet, L., 2015, The geological signature of a
1020 slab tear below the Aegean: Tectonophysics, v. 659, p. 166-182.

1021 Kahle, H.-G., Cocard, M., Peter, Y., Geiger, A., Reilinger, R., McClusky, S., King, R., Barka, A., and Veis,
1022 G., 1999, The GPS strain rate field in the Aegean Sea and western Anatolia: Geophysical Research
1023 Letters, v. 26, no. 16, p. 2513-2516.

1024 Kahler, F., 1987, Fusuliniden-Faunen auf Chios, Kalymnos und Kos in der Aegaeis: Mitteilungen der
1025 Österreichischen Geologischen Gesellschaft, v. 80, p. 287-323.

1026 Karacık, Z., Yılmaz, Y., Pearce, J. A., and Ece, Ö. I., 2008, Petrochemistry of the south Marmara
1027 granitoids, northwest Anatolia, Turkey: International Journal of Earth Sciences, v. 97, no. 6, p.
1028 1181-1200.

1029 Katagas, C., and Sapountzis, E., 1977, Petrochemistry of low and medium grade mafic metamorphic
1030 rocks from Leros island, Greece: Tschermaks mineralogische und petrographische Mitteilungen,
1031 v. 24, no. 1-2, p. 39-55.

1032 Katagas C.G., 1980, Metamorphic Zones and Physical Conditions of Metamorphism in Leros Island,
1033 Greece. Contributions to Mineralogy and Petrology, v. 73, p. 389-402.

1034 Katsikatsos, G., Mataragas, D., Migiros, G., and Triandaphyllis, E., 1982, Geological Study of Lesbos
1035 Island. Special Report. I.G.M.E., Athens (Greece), 93 p.

1036 Kissel, C., and Laj, C., 1988, The Tertiary geodynamical evolution of the Aegean arc: a paleomagnetic
1037 reconstruction: Tectonophysics, v. 146, no. 1, p. 183-201.

1038 Kobayashi, F., and Altiner, D., 2008, Late Carboniferous and early Permian fusulinoideans in the central
1039 Taurides, Turkey: biostratigraphy, faunal composition and comparison: Journal of Foraminiferal
1040 Research, v. 38, no. 1, p. 59-73.

1041 Koepke, J., Seidel, E., and Kreuzer, H., 2002, Ophiolites on the Southern Aegean islands Crete,
1042 Karpathos and Rhodes: composition, geochronology and position within the ophiolite belts of
1043 the Eastern Mediterranean: Lithos, v. 65, no. 1, p. 183-203.

1044 Kotopouli, C. N., Pe-Piper, G., and Piper, D. J. W., 2000, Petrology and evolution of the Hercynian Pieria
1045 Granitoid Complex (Thessaly, Greece): paleogeographic and geodynamic implications: Lithos, v.
1046 50, no. 1, p. 137-152.

1047 Koutsovitis, P., Soukis, K., Voudouris, P., Lozios, S., Ntaflos, T., Stouraiti, C., and Koukouzas, N., 2021,
1048 The Late Cretaceous magmatic arc of the south Aegean: Geodynamic implications from
1049 petrological and geochemical studies of granitoids from Anafi island (Cyclades - Greece):
1050 International Geology Review. doi 10.1080/00206814.2021.1884906.

1051 Le Pichon, X., and Angelier, J., 1979, The Hellenic Arc and Trench system: a key to the neotectonic
1052 evolution of the eastern Mediterranean area: Tectonophysics, v. 69, p. 1-42.

1053 Lekkas, E., Danamos, G., Skourtsos, E., and Sakellariou, D., 2002, Position of the middle Triassic Tyros-
1054 beds in the Gavrovo-Tripolis unit (Rhodes island, Ddecanese, Greece): Geologica Carpathica, v.
1055 53, no. 1, p. 37-44.

1056 Labrousse, L., Huet, B., Le Pourhiet, L., Jolivet, L., and Burov, E., 2016, Rheological implications of
1057 extensional detachments: Mediterranean and numerical insights: Earth-Science Reviews, v. 161,
1058 p. 233-258.

1059 Lister, G. S., Banga, G., and Feenstra, A., 1984, Metamorphic core complexes of Cordilleran type in the
1060 Cyclades, Aegean Sea, Greece: Geology, v. 12, no. 4, p. 221-225.

1061 Mandl, G., 1987, Tectonic deformation by rotating parallel faults; the "bookshelf" mechanism:
1062 Tectonophysics, v. 141, no. 4, p. 277-316.

1063 Martha, S. O., Dörr, W., Gerdes, A., Krahl, J., Linckens, J., and Zulauf, G., 2017, The tectonometamorphic
1064 and magmatic evolution of the Uppermost Unit in central Crete (Melambes area): constraints
1065 on a Late Cretaceous magmatic arc in the Internal Hellenides (Greece): Gondwana Research, v.
1066 48, p. 50-71.

1067 McClusky, S. C., Balassanian, S., Barka, A., Demir, C., Erginta V, S., Georgiev, I., Gurkan, O., Hamburger,
1068 M., Hurst, K., Kahle, H., Kastens, K., Ke kelidze, G., King, R., Kotzev, V., Lenk, O., Mahmoud, S.,
1069 Mishin, A., Nadariya, M., Ouzounis, A., Paradissis, D., Peter, Y., Prilepin, M., Reilinger, R., Sanli,
1070 I., Seeger, H., Tealeb, A., Toksuez, M. N., and Veis, G., 2000, Global Positioning System
1071 constraints on plate kinematics and dynamics in the eastern Mediterranean and Caucasus:
1072 Journal of Geophysical Research, v. 105, no. (B3), p. 5695-5719.

1073 Meinhold, G., Reischmann, T., Kostopoulos, D., Lehnert, O., Matukov, D., and Sergeev, S., 2008,
1074 Provenance of sediments during subduction of Palaeotethys: Detrital zircon ages and olistolith
1075 analysis in Palaeozoic sediments from Chios Island, Greece: Palaeogeography Palaeoclimatology
1076 Palaeoecology, v. 263, p. 71-91.

1077 Menant, A., Sternai, P., Jolivet, L., Guillou-Frottier, L., and Gerya, T., 2016, 3D numerical modeling of
1078 mantle flow, crustal dynamics and magma genesis associated with slab roll-back and tearing:
1079 The eastern Mediterranean case: Earth and Planetary Science Letters, v. 442, p. 93-107.

1080 Mountrakis, D., 1986, The Pelagonian Zone in Greece: A Polyphase-Deformed Fragment of the
1081 Cimmerian Continent and Its Role in the Geotectonic Evolution of the Eastern Mediterranean:
1082 The Journal of Geology, v. 94, no. 3, p. 335-347.

1083 Mutti, E., Orombelli, G. and Pozzi, R., 1970, Geological studies of the Dodecanese Islands (Aegean Sea).
1084 Geological map of the Island of Rhodes and Explanatory Notes: Annales Géologiques des Pays
1085 Helléniques, v. 22, p. 77-226.

1086 Oberhänsli, R., Candan, O., Dora, O. Ö., and Dürr, S. H., 1997, Eclogites within the Menderes
1087 Massif/western Turkey: Lithos, v. 41, no. 1, p. 135-150.

1088 Oberhänsli, R., Monié, P., Candan, O., Warkus, F. C., Partzsch, J. H., and Dora, O. Ö., 1998, The age of
1089 blueschist metamorphism in the Mesozoic cover series of the Menderes Massif: Schweizerische
1090 Mineralogische and Petrographische Mitteilungen, v. 78, p. 309-316.

1091 Okay, A., 1989, Geology of the Menderes Massif and the Lycian Nappes south of Denizli, western
1092 Taurides: Bulletin of the Mineral Research and Exploration, v. 109, p. 37-51.

1093 Okay, A. I., Harris, N. B. W., and Kelley, S. P., 1998, Exhumation of blueschists along a Tethyan suture
1094 in northwest Turkey: Tectonophysics, v. 285, no. 3, p. 275-299.

1095 Okay, A., and Whitney, D., 2010, Blueschists, eclogites, ophiolites and suture zones in northwest
1096 Turkey: a review and a field excursion guide: Ofioliti, v. 35, p. 131-172.

1097 Okay, A. I., and Topuz, G., 2017, Variscan orogeny in the Black Sea region: International Journal of Earth
1098 Sciences, v. 106, no. 2, p. 569-592.

1099 Papanikolaou, D., and Sideris, C., 1983, Le Paléozoïque de l'autochtone de Chios: une formation à blocs
1100 de types wildflysch d'âge Permien (pro parte): Comptes Rendus de l'Académie des Sciences, v.
1101 297, p. 603-606.

1102 Papanikolaou, D., and Demirtasli, E., 1987, Geological correlations between the alpine segments of the
1103 Hellenides-Balkanides and Taurides-Pontides, in Flügel, H. W., Sassi, F. P., and Grecula, P., eds.,

1104 Pre-Variscan and Variscan Events in the Alpine Mediterranean Mountain Belts: Bratislava,
1105 Mineralia Slovaca, Monography, p. 387-396.

1106 Papanikolaou, D., 1997, The tectonostratigraphic terranes of the Hellenides: Annales Géologiques des
1107 Pays Helléniques, v. 37.

1108 Papanikolaou, D., 2013, Tectonostratigraphic models of the Alpine terranes and subduction history of
1109 the Hellenides: Tectonophysics, v. 595-596, p. 1-24.

1110 Passchier, C. W., and Trouw, R. A. J., 2005, Microtectonics, Berlin, Springer-Verlag, 366 p.

1111 Patzak, M., Okrusch, M., and Kreuzer, H., 1994, The Akrotiri unit on the island of Tinos, Cyclades,
1112 Greece: witness of a lost terrane of Late Cretaceous age.: Neues Jahrbuch für Geologie und
1113 Palaeontologie, v. 194, p. 211-252.

1114 Pe-Piper, G., and Piper, D. J. W., 2002, The igneous rocks of Greece, Berlin, Borntraeger, Beiträge zur
1115 regionalen Geologie der Erde, 573 p.

1116 Piromallo, C., and Morelli, A., 2003, P wave tomography of the mantle under the Alpine-Mediterranean
1117 area: Journal of Geophysical Research: Solid Earth, v. 108, no. B2 2065,
1118 doi:10.1029/2002JB001757.

1119 Poulaki, E. M., Stockli, D. F., Flansburg, M. E., and Soukis, K., 2019, Zircon U-Pb Chronostratigraphy and
1120 provenance of the Cycladic Blueschist Unit and the nature of the contact with the Cycladic
1121 Basement on Sikinos and Ios Islands, Greece: Tectonics, v. 38, no. 10, p. 3586-3613.

1122 Pourteau, A., Candan, O., and Oberhänsli, R., 2010, High-pressure metasediments in central Turkey:
1123 Constraints on the Neotethyan closure history: Tectonics, v. 29, no. 5, p. TC5004.

1124 Pourteau, A., Sudo, M., Candan, O., Lanari, P., Vidal, O., Oberhänsli, R., 2013, Neotethys closure history
1125 of Anatolia: insights from ^{40}Ar-^{39}Ar geochronology and P-T estimation in high-pressure
1126 metasedimentary rocks: Journal of Metamorphic Geology, v. 31, p. 585-606.

1127 Rigo, A., Lyon-Caen, H., Armijo, R., Deschamps, A., Hatzfeld, D., Makropoulos, K., Papadimitriou, P.,
1128 and Kassaras, I., 1996, A microseismic study in the western part of the Gulf of Corinth (Greece):
1129 implications for large-scale normal faulting mechanisms: Geophysical Journal International, v.
1130 126, no. 3, p. 663-688.

1131 Rimmelé, G., Jolivet, L., Oberhänsli, R., and Goffé, B., 2003, Deformation history of the high-pressure
1132 Lycian Nappes and implications for tectonic evolution of SW Turkey: Tectonics, v. 22, no. 2, p.
1133 doi:10.1029/2001TC901041.

1134 Rimmelé, G., Parra, T., Goffé, B., Oberhansli, R., Jolivet, L., and Candan, O., 2005, Exhumation Paths of
1135 High-Pressure-Low-Temperature Metamorphic Rocks from the Lycian Nappes and the Menderes
1136 Massif (SW Turkey): a Multi-Equilibrium Approach: J. Petrology, v. 46, no. 3, p. 641-669.

1137 Rimmelé, G., Oberhänsli, R., Candan, O., Goffé, B., and Jolivet, L., 2006, The wide distribution of HP-LT
1138 rocks in the Lycian Belt (Western Turkey): implications for accretionary wedge geometry:
1139 Geological Society, London, Special Publications, v. 260, no. 1, p. 447-466.

1140 Ring, U., Gessner, K., Güngör, T., and Passchier, C. W., 1999a, The Menderes Massif of western Turkey
1141 and the Cycladic Massif in the Aegean—do they really correlate?: Journal of the Geological
1142 Society, v. 156, no. 1, p. 3-6.

1143 Ring, U., Laws, S., and Bernet, M., 1999b, Structural analysis of a complex nappe sequence and late-
1144 orogenic basins from the Aegean Island of Samos, Greece: Journal of Structural Geology, v. 21,
1145 no. 11, p. 1575-1601.

1146 Ring, R., Brachert, T., and Fassoulas, C., 2001, Middle Miocene graben development in Crete and its
1147 possible relation to large-scale detachment faults in the southern Aegean: Terra Nova, v. 13, no.
1148 4, p. 297-304.

1149 Ring, U., and Layer, P. W., 2003, High-pressure metamorphism in the Aegean, eastern Mediterranean:
1150 Underplating and exhumation from the Late Cretaceous until the Miocene to Recent above the
1151 retreating Hellenic subduction zone: Tectonics, v. 22, no. 3, p. 1022,
1152 doi:1010.1029/2001TC001350.

1153 Ring, U., Johnson, C., Hetzel, R., and Gessner, K., 2003, Tectonic denudation of a Late Cretaceous-
1154 Tertiary collisional belt: regionally symmetric cooling patterns and their relation to extensional
1155 faults in the Anatolide belt of western Turkey: Geological Magazine, v. 140, no. 04, p. 421-441.

1156 Ring, U., Glodny, J., Will, T., and Thomson, S., 2010, The Hellenic subduction system: High-pressure
1157 metamorphism, exhumation, normal faulting, and large-scale extension: Annual Review of Earth
1158 and Planetary Sciences, v. 38, no. 1, p. 45-76.

1159 Ring, U., Glodny, J., Will, T. M., and Thomson, S., 2011, Normal faulting on Sifnos and the South Cycladic
1160 Detachment System, Aegean Sea, Greece: Journal of the Geological Society, v. 168, no. 3, p. 751-
1161 768.

1162 Ring, U., Gessner, K., and Thomson, S., 2017, Variations in fault-slip data and cooling history reveal
1163 corridor of heterogeneous backarc extension in the eastern Aegean Sea region: Tectonophysics,
1164 v. 700-701, p. 108-130.

1165 Robertson, A. H. F., Clift, P. D., Degnan, P. J., and Jones, G., 1991, Palaeogeographic and palaeotectonic
1166 evolution of the Eastern Mediterranean Neotethys: Palaeogeography, Palaeoclimatology,
1167 Palaeoecology, v. 87, no. 1, p. 289-343.

1168 Robertson, A., Ustaömer, T., 2009, Formation of the Late Palaeozoic Konya Complex and comparable
1169 units in southern Turkey by subduction-accretion processes: Implications for the tectonic
1170 development of Tethys in the Eastern Mediterranean region: Tectonophysics, v. 473, p. 113-148.

1171 Roche, V., Conand, C., Jolivet, L., and Augier, R., 2018, Tectonic evolution of Leros (Dodecanese,
1172 Greece) and correlations between the Aegean Domain and the Menderes Massif: Journal of the
1173 Geological Society, v. 175, no. 5, p. 836-849.

1174 Roche, V., Jolivet, L., Papanikolaou, D., Bozkurt, E., Menant, A., and Rimmelé, G., 2019, Slab
1175 fragmentation beneath the Aegean/Anatolia transition zone: Insights from the tectonic and
1176 metamorphic evolution of the Eastern Aegean region: Tectonophysics, v. 754, p. 101-129.

1177 Salaün, G., Pedersen, H. A., Paul, A., Farra, V., Karabulut, H., Hatzfeld, D., Papazachos, C., Childs, D. M.,
1178 Pequegnat, C., and Team, S., 2012, High-resolution surface wave tomography beneath the
1179 Aegean-Anatolia region: constraints on upper-mantle structure: Geophysical Journal
1180 International, v. 190, no. 1, p. 406-420.

1181 Schmid, S. M., Fügenschuh, B., Kounov, A., Maţenco, L., Nievergelt, P., Oberhänsli, R., Pleuger, J.,
1182 Schefer, S., Schuster, R., Tomljenović, B., Ustaszewski, K., and van Hinsbergen, D. J. J., 2020,
1183 Tectonic units of the Alpine collision zone between Eastern Alps and western Turkey: Gondwana
1184 Research, v. 78, p. 308-374.

1185 Schneider, D. A., Grasemann, B., Lion, A., Soukis, K., and Draganits, E., 2018, Geodynamic significance
1186 of the Santorini Detachment System (Cyclades, Greece): Terra Nova, v. 30, no. 6, p. 414-422.

1187 Seidel, E., Kreuzer, H., and Harre, W., 1982, A late Oligocene/early Miocene high pressure belt in the
1188 External Hellenides: Geologisches Jahrbuch, v. E23, p. 165-206.

1189 Şengör, A. M. C., and Yilmaz, Y., 1981, Tethyan evolution of Turkey: A plate tectonic approach:
1190 Tectonophysics, v. 75, no. 3-4, p. 181-241.

1191 Şengör, A. M. C., Satir, M., and Akkök, R., 1984a, Timing of tectonic events in the Menderes Massif,
1192 western Turkey: Implications for tectonic evolution and evidence for pan-African basement in
1193 Turkey: Tectonics, v. 3, no. 7, p. 693-707.

1194 Şengör, A. M. C., Yılmaz, Y., and Sungurlu, O., 1984b, Tectonics of the Mediterranean Cimmerides:
1195 nature and evolution of the western termination of Palaeo-Tethys: Geological Society, London,
1196 Special Publications, v. 17, no. 1, p. 77-112.

1197 Sözbilir, H., Sarı, B., Uzel, B., Sümer, Ö., and Akkiraz, S., 2011, Tectonic implications of transtensional
1198 supradetachment basin development in an extension-parallel transfer zone: the Kocaçay Basin,
1199 western Anatolia, Turkey: Basin Research, v. 23, no. 4, p. 423-448.

1200 Stampfli, G., Marcoux, J., and Baud, A., 1991, Tethyan margins in space and time: Palaeogeography,
1201 Palaeoclimatology, Palaeoecology, v. 87, no. 1, p. 373-409.

1202 Stampfli, G. M., and Borel, G. D., 2002, A plate tectonic model for the Paleozoic and Mesozoic
1203 constrained by dynamic plate boundaries and restored synthetic oceanic isochrons: Earth and
1204 Planetary Science Letters, v. 196, no. 1-2, p. 17-33.

1205 Stampfli, G. M., Vavassis, I., De Bono, A., Rosselet, F., Matti, B., and Bellini, M., 2003, Remnants of the
1206 Paleotethys oceanic suture-zone in the western Tethyan area. Stratigraphic and structural
1207 evolution on the Late Carboniferous to Triassic continental and marine successions in Tuscany
1208 (Italy): Regional reports and general correlation: Bolletino della Società Geologica Italiana, v. 2,
1209 p. 1-24.

1210 Sternai, P., Jolivet, L., Menant, A., Gerya, T., 2014, Driving the upper plate surface deformation by slab
1211 rollback and mantle flow: Earth and Planetary Science Letters, v. 405, p. 110-118.

1212 Thorbecke, G., 1987, Zur Zonengliederung der ägäischen Helleniden und westlichen Tauriden,
1213 Gesellschaft der Geologie- und Bergbaustudenten in Österreich, v. SH2, p. 1-161.

1214 Tomaschek, F., Keiter, M., Kennedy, A. K., and Ballhaus, C., 2008, Pre-Alpine basement within the
1215 Northern Cycladic Blueschist Unit on Syros Island, Greece: Zeitschrift der Deutschen Gesellschaft
1216 für Geowissenschaften, v. 159, no. 3, p. 521-5232.

1217 Triantaphyllis, M. B., and Karfakis, I., 1994, The geological and tectonics structure of the Kalymnos
1218 island (Dodecanese): Bulletin of the Geological Society of Greece, v. XXX, no. 2, p. 123-134.

1219 Tselepides V., and Carras, N., 2013, Internal report on the results of the field-work on Kalymnos Island,
1220 IGME Library number E11930, 13pp.

1221 Ustaömer, P. A., Ustaömer, T., Collins, A. S., and Reischpeitsch, J., 2009, Lutetian arc-type magmatism
1222 along the southern Eurasian margin: New U-Pb LA-ICPMS and whole-rock geochemical data from
1223 Marmara Island, NW Turkey: Mineralogy and Petrology, v. 96, no. 3, p. 177-196.

1224 Uzel, B., Langereis, C. G., Kaymakci, N., Sözbilir, H., Özkaymak, Ç., and Özkaptan, M., 2015,
1225 Paleomagnetic evidence for an inverse rotation history of Western Anatolia during the
1226 exhumation of Menderes core complex: Earth and Planetary Science Letters, v. 414, p. 108-125.

1227 van Hinsbergen, D. J. J., Hafkenscheid, E., Spakman, W., Meulenkamp, J. E., and Wortel, R., 2005a,
1228 Nappe stacking resulting from subduction of oceanic and continental lithosphere below Greece:
1229 Geology, v. 33, no. 4, p. 325-328.

1230 van Hinsbergen, D. J. J., Langereis, C. G., and Meulenkamp, J. E., 2005b, Revision of the timing,
1231 magnitude and distribution of Neogene rotations in the western Aegean region: Tectonophysics,
1232 v. 396, no. 1-2, p. 1-34.

1233 van Hinsbergen, D. J. J., and Boekhout, F., 2009, Neogene brittle detachment faulting on Kos (E Greece):
1234 implications for a southern break-away fault of the Menderes metamorphic core complex
1235 (western Turkey): Geological Society, London, Special Publications, v. 311, no. 1, p. 311-320.

1236 van Hinsbergen, D. J. J., 2010, A key extensional metamorphic complex reviewed and restored: The
1237 Menderes Massif of western Turkey: Earth-Science Reviews, v. 102, no. 1-2, p. 60-76.

1238 Vavassis, I., De Bono, A., Stampfli, G. M., Giorgis, D., Valloton, A., and Amelin, Y., 2000, U-Pb and Ar-Ar
1239 geochronological data from Pelagonian basement in Evia (Greece): geodynamic implications for
1240 the evolution of the Palaeotethys Schweizerische Mineralogische and Petrographische
1241 Mitteilungen, v. 80, p. 21-43.

1242 Wernicke, B., 1981, Low-angle normal faults in the Basin and Range Province-Nappe tectonics in an
1243 extending orogen: Nature, v. 291, p. 645-648.

1244 Wolfe, M. R., and Stockli, D. F., 2010, Zircon (U-Th)/He thermochronometry in the KTB drill hole,
1245 Germany, and its implications for bulk He diffusion kinetics in zircon: Earth and Planetary Science
1246 Letters, v. 295, no. 1, p. 69-82.

1247 Xypolias, P., Iliopoulos, I., Chatzaras, V., and Kokkalas, S., 2012, Subduction- and exhumation-related
1248 structures in the Cycladic Blueschists: Insights from south Evia Island (Aegean region, Greece):
1249 Tectonics, v. 31, no. 2, p. TC2001.

1250 Zanchi, A., Garzanti, E., Larghi, C., Angiolini, L., and Gaetani, M., 2003, The Variscan orogeny in Chios
1251 (Greece): Carboniferous accretion along a Palaeotethyan active margin: Terra Nova, v. 15, no. 3,
1252 p. 155.162.

1253 Zulauf, G., Klein, T., Kowalczyk, G., Krahl, J., and Romano, S. S., 2008, The Mirsini Syncline of eastern
1254 Crete, Greece: a key area for understanding pre-Alpine and Alpine orogeny in the eastern

Mediterranean: Zeitschrift der Deutschen Gesellschaft für Geowissenschaften, v. 159 no. 3, p. 399-414.

Zulauf, G., Dörr, W., Marko, L., and Krahl, J., 2018, The late Eo-Cimmerian evolution of the external Hellenides: constraints from microfabrics and U-Pb detrital zircon ages of Upper Triassic (meta)sediments (Crete, Greece): International Journal of Earth Sciences, v. 107, no. 8, p. 2859-2894.

Zulauf, G., Dörr, W., Xypolias, P., Gerdes, A., Kowalczyk, G., and Linckens, J., 2019, Triassic evolution of the western Neotethys: constraints from microfabrics and U-Pb detrital zircon ages of the Plattenkalk Unit (External Hellenides, Greece): International Journal of Earth Sciences, v. 108, no. 8, p. 2493-2529.

Figure captions

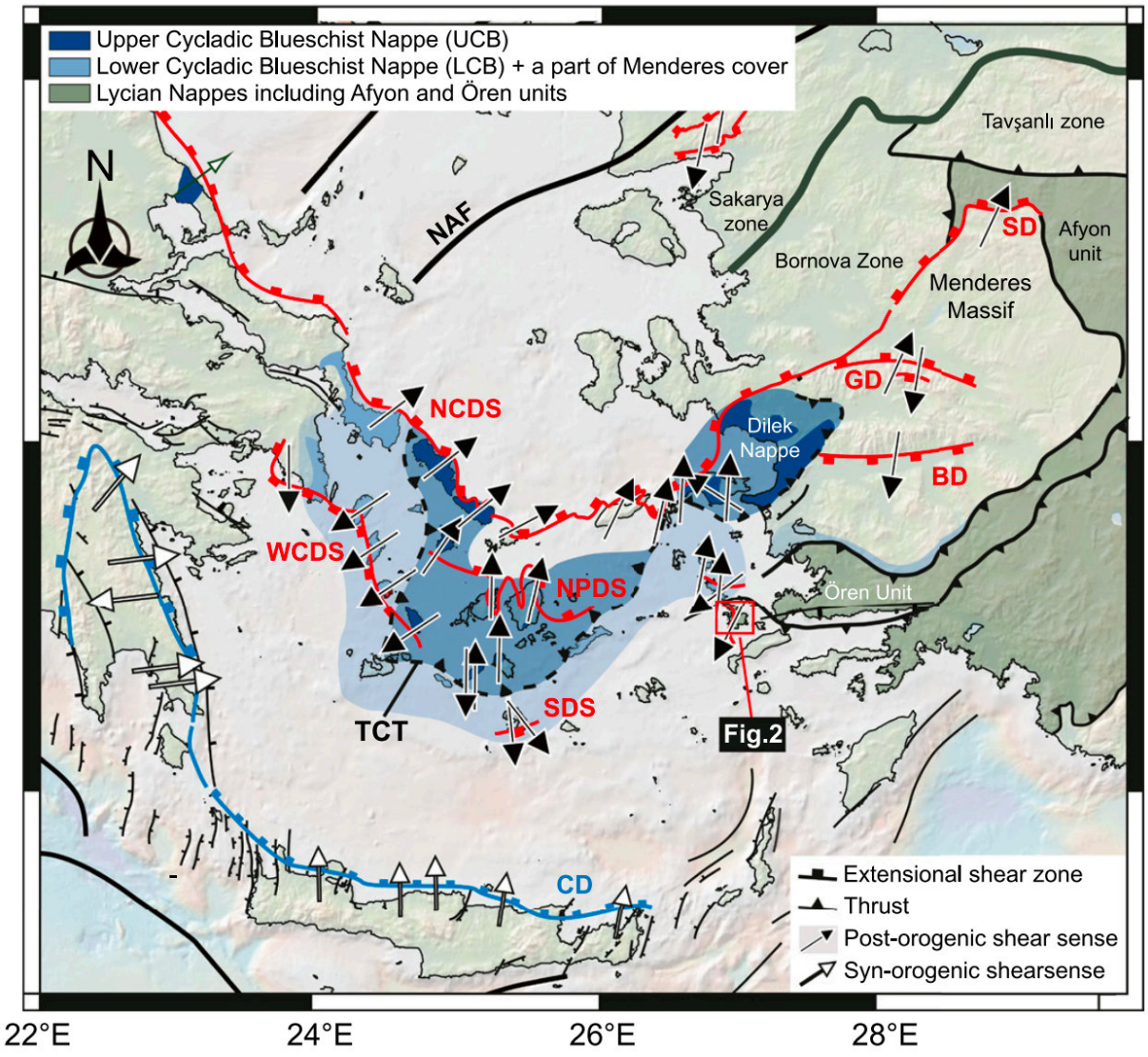

Figure 1: Tectonic map of the Aegean region showing the kinematics of the major Cenozoic faults including syn- and post-orogenic shear sense (modified after Jolivet et al., 2013; Rimmelé et al., 2006; Roche et al., 2018). BD: Büyük Menderes Detachment, CD: Cretan Detachment, GD: Gediz Menderes Detachment, NAF: North Anatolian Fault, NCDS: North Cycladic Detachment System, NPDS: Naxos-Paros Extensional Fault System, SD: Simav Detachment, SDS: Santorini Detachment System, TCT: Trans-Cycladic Thrust, WCDS: West Cycladic Detachment System.

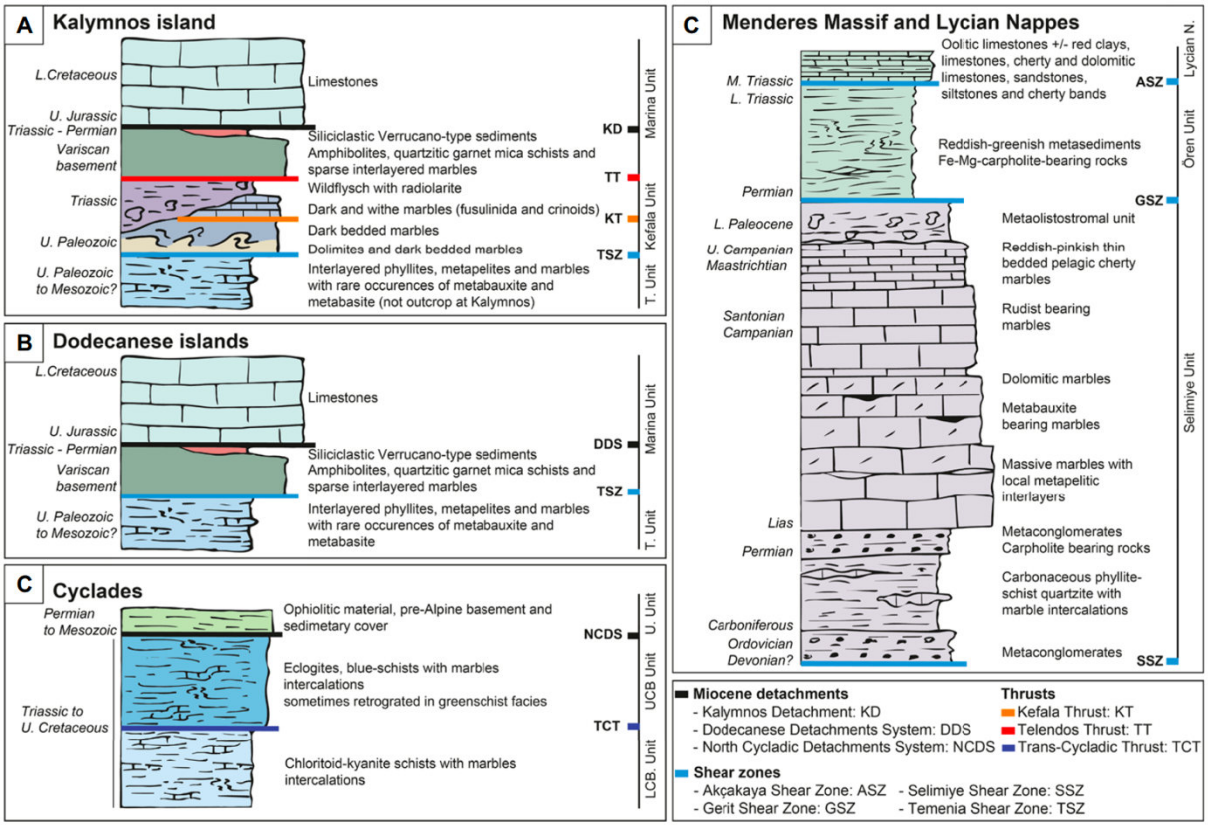

Figure 2: Simplified tectono-stratigraphic sequences from a) Kalymnos, b) the Dodecanese islands, c) the Cyclades and d) the Menderes area (based on this study and modified from Roche et al. (2019). L: Lower, LCB: Lower Cycladic Blueschist, M: Middle, N: Nappes, T: Temenia, U: Upper, UCB: Upper Cycladic Blueschist.

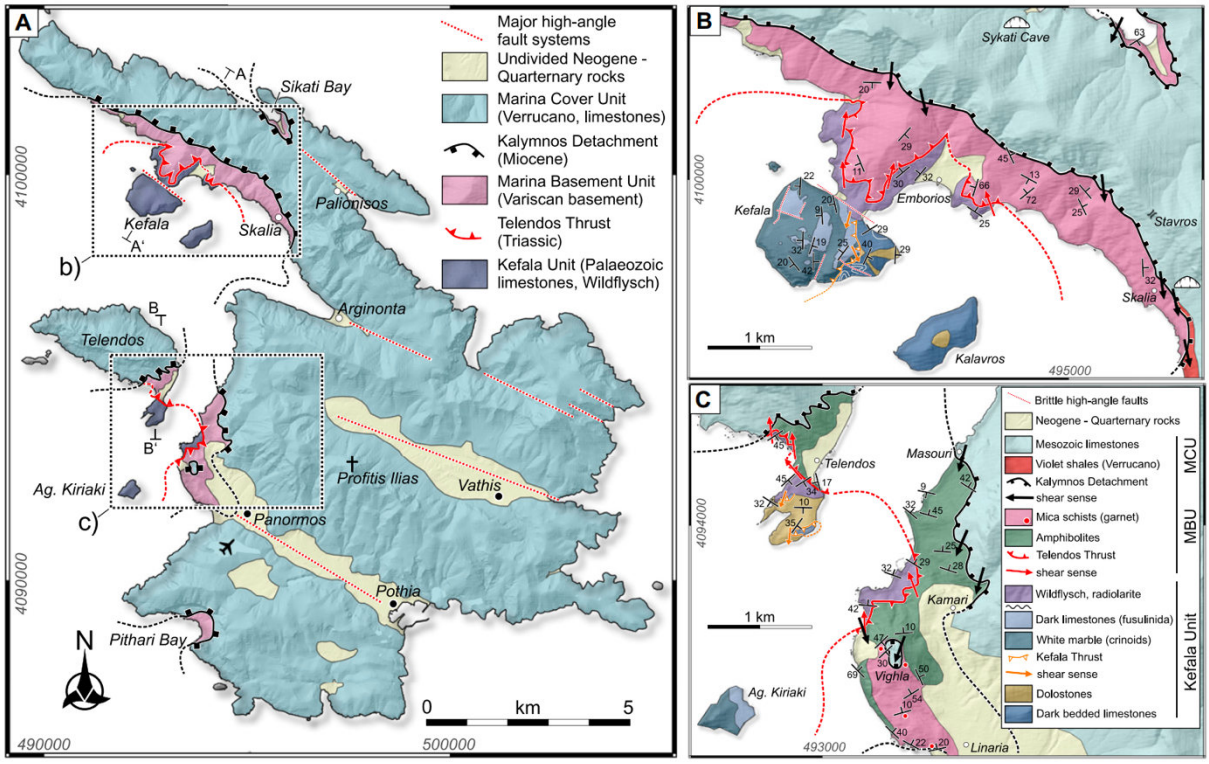

1279

1280 Figure 2: New geological map of Kalymnos and Telendos islands, Dodecanese archipelago. A-A' and B-

1281 B' indicate location of cross sections shown in Figure 3. MBU: Marina Basement Unit, MCU:

1282 Marina Cover Unit.

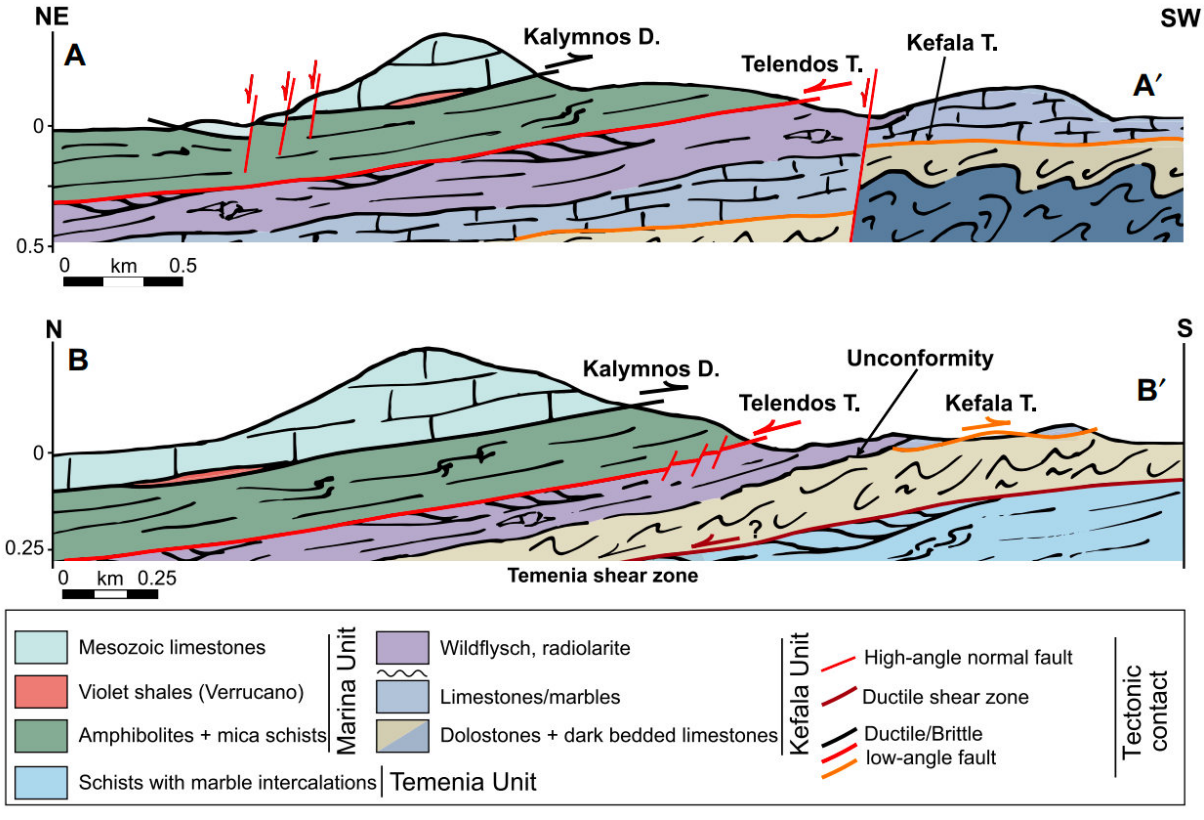

1283

1284 Figure 3: Cross sections A-A' and B-B' (note different scales). Locations indicated in Figure 2.

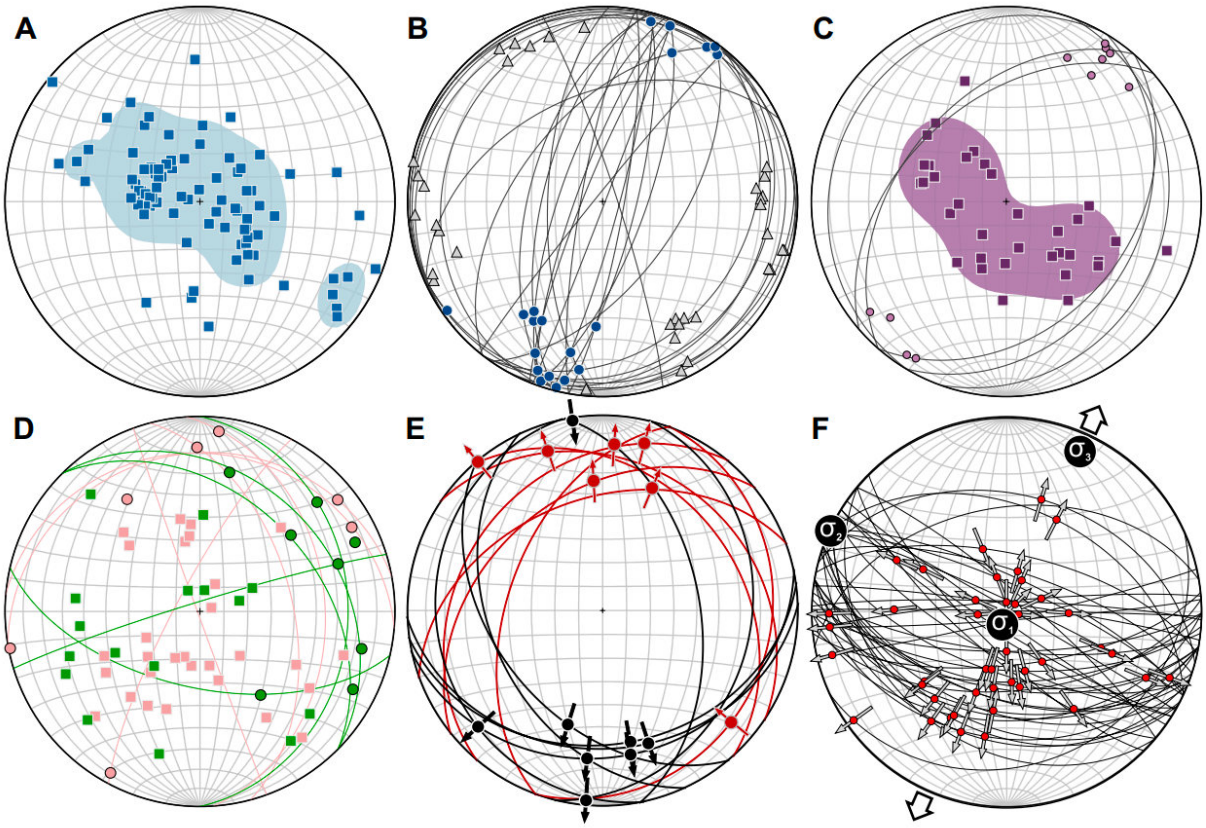

Figure 4: Schmidt nets (Lambert azimuthal equal-area projection, lower hemisphere) of structural field data. Contours represent 2σ from a uniform distribution (exponential Kamb). a) and b) Paleozoic limestones/marbles of the Kefala Unit below angular unconformity: blue squares: poles to bedding, blue great circles: axial planes of folds, blue circles: fold axes, grey triangles: poles to joints. c) Wildflysch (olistostrome/congomerates/radiolarites) of the Kefala Unit above the angular unconformity: purple squares: poles to bedding, purple great circles: axial planes of folds, purple circles: fold axes. d) Amphibolite (green) and quartz-micaschists (pink) of the Marina Unit: squares: poles to foliation, great circles: axial planes of folds, circles: fold axes. e) Fault planes (great circles) and lineation/striation with kinematic (displacement of the hanging wall) of the Telendos Thrust (red) and the Kalymnos Detachment (black). f) Angelier plot of high angle faults. Stress state (σ1> σ2> σ3): 200/83, 294/00, 024/07.

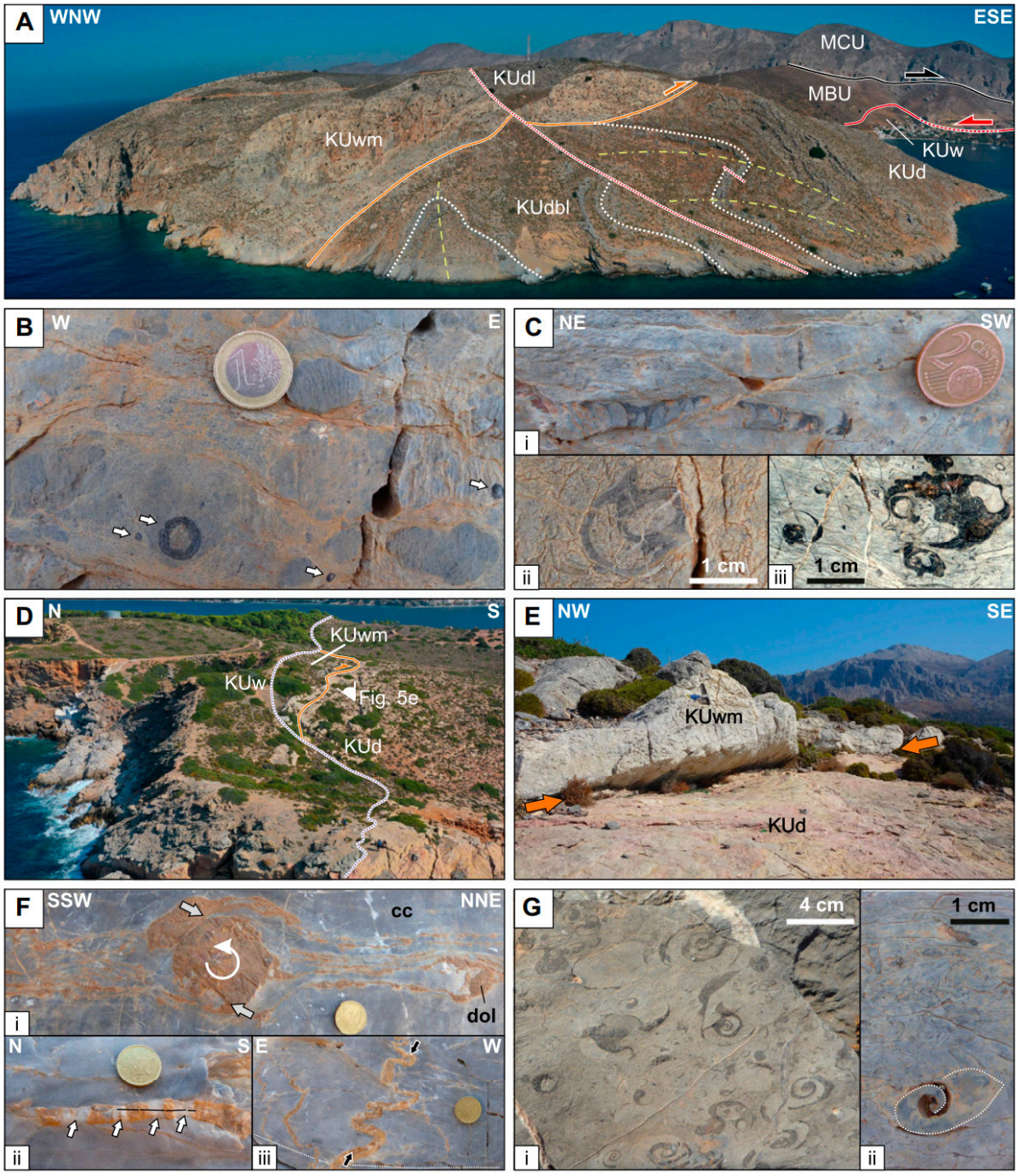

1297

1298 Figure 5: a) Drone panorama of the south coast of Kefala (492926E, 4098870N, 60 m a.s.l.). KUdbl: dark
1299 bedded limestone of the Kefala Unit; KUd: dolostone of the Kefala Unit; KUwm: white marbles
1300 of the Kefala Unit; KUdl: dark limestone of the Kefala Unit; KUw: wildflysch of the Kefala Unit;
1301 MBU: Variscan crystalline of the Marina Basement Unit; MCU: Mesozoic limestones of the
1302 Marina Cover Unit; orange line: Kefala Thrust; red line: Telendos Thrust; black line: Kalymnos
1303 Detachment; red dotted line: high angle faults; white dotted line: trace of selected bedding
1304 outlining the refold structure in the dark bedded limestones of the Kefala Unit; yellow dashed
1305 line: trace of first axial plane; yellow dashed-dotted line: traces of second axial plane. b) Cross-
1306 section through basal part of the aboral cup of a crinoid surrounded by several columnals (white

arrows) in nodular limestones in the dark bedded limestones of the Kefala Unit (493057E, 4133998N). c) Fossils in the dark bedded limestones of the Kefala Unit: (i): Internal mold (subcentral longitudinal section) of a poorly preserved orthocone nautiloid with chambers that are partially filled with cement. The outer wall of the cephalopod is partly dissolved. (493114E, 4099520N). (ii): Section of an isotrophic to rarely slightly asymmetric coiled bellerophontid gastropod (493068E, 4099408N). (iii): bellerophontid shell debris (493114E, 4099520N). d) Drone picture of the angular unconformity (dotted line) of the wildflysch of the Marina Unit (KUw) sealing the Kefala Trust (orange line), which juxtaposes the white marbles (KUwm) on top of the dolostones (KUd) of the Kefala Unit (Telendos, 492500E, 4094259N, 25 m a.s.l.). View direction of Figure 5e is indicated. e) Kefala Thrust displacing the white marbles (KUwm) on top of the dolostones (KUd) of the Kefala Unit (Telendos, 492621E, 4094234N). f) Mylonitic bluish-white calcite (cc) marbles of the Kefala Unit (mylonitic foliation sm 258/22, mylonitic stretching lineation lm 194/05, 492751E, 4099734N): (i): Section parallel lm and perpendicular to sm. Brownish dolomite layers (dol) are cataclastically fractured but form coherent pinch-and-swell boudinage, which are potentially rotated into the shear direction forming winged inclusions (grey arrows indicate embayment of the winged inclusion; white circular arrow shows the sense of rotation). (ii): Section parallel lm and perpendicular to sm. Torn blocky boudinage. Note the white precipitated calcite in the interboudin zone (stretch s = 1.58). (iii): Section perpendicular to lm. White dotted line outlines trace of sm. Ptygmatic folding of dol veins with fold axis parallel to lm and axial planes roughly parallel to sm indicate strong layer parallel shortening during shearing indicative of general shear deformation (s = 0.55). g) Gastropod shell bed in the dark limestones of the Kefala Unit. (i): Bedding plane (128/22) with densely packed globose gastropods (492835E, 4099276E). (ii): fine grained shell bank with a gastropod mold (492839E, 4099600E).

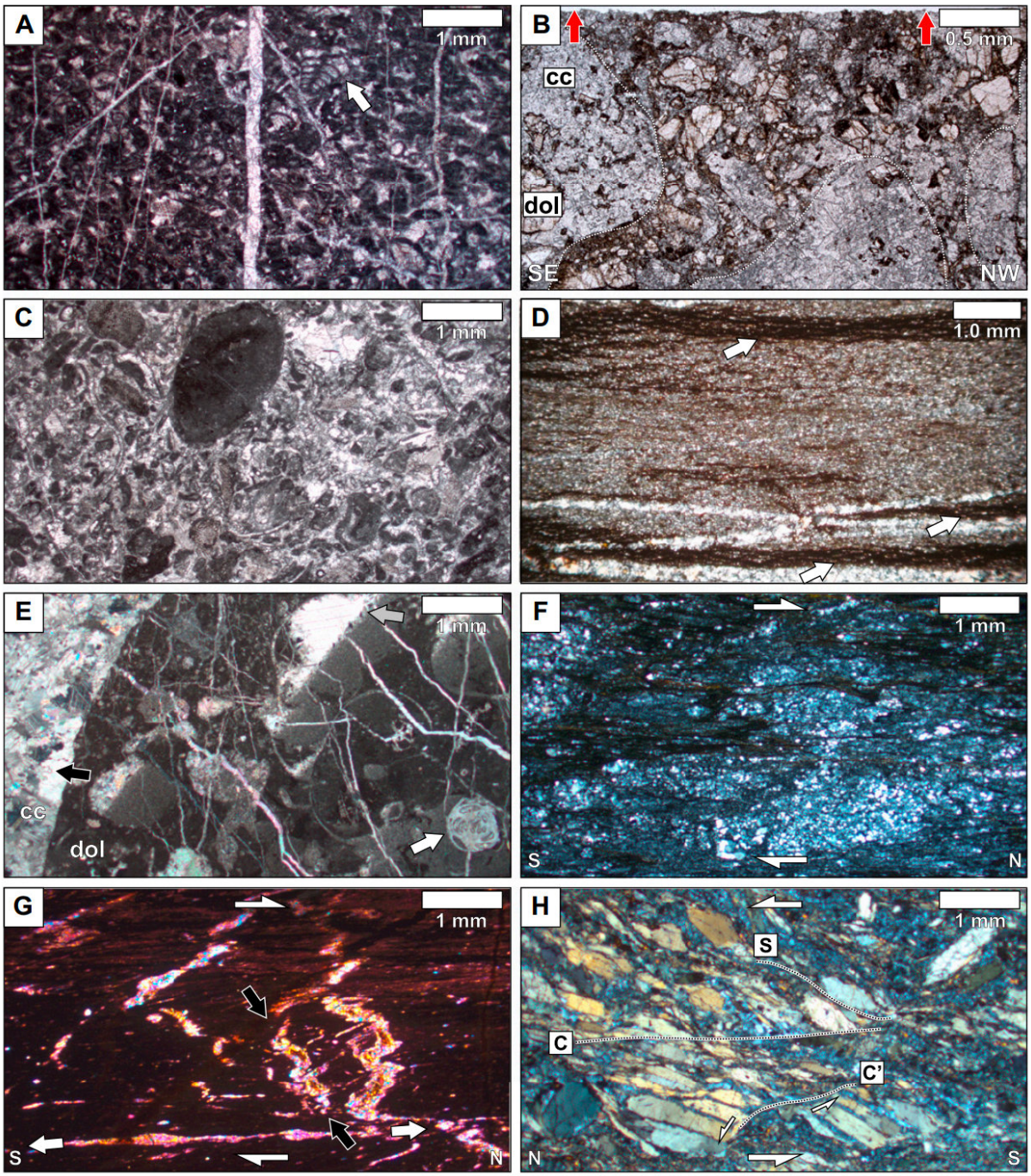

Figure 6: Thin sections in plane (PPL) and cross polarized light (XPL). a) Peletoidal packstone-grainstone with paleotextulariid foraminifera (arrow) (PPL, 493052E, 4099247N). b) Dolomite (dol)/calcite (cc) cataclastic fault rocks of the Kefala Thrust shown in Figure 5a (PPL, 492943E, 4099233N). Red arrows mark the slickenside of the fault. White dotted line shows the irregular contact between different generations of cataclasites. c) Crinoidal grainstone containing rare mollusk debris and foraminifera (PPL, 492524E, 4099840N). d) Deformed radiolarite layers of the wildflysch subunit consists of fine-grained (<10 µm) quartz with small amount of calcite. Deformation and folding of these layers are accommodated by dissolution-precipitation processes and development of a spaced pressure solution cleavage (white arrows). The thin

section is from the sample K43, which was collected close to the Telendos Thrust for white mica $^{40}Ar/^{39}Ar$ dating from the cleavage domains (PPL, 493499E, 4093211N). e) Thin section of the margin of a dolomite (dol) component in the calcite (cc) marble block in the wildflysch (see Fig. 7b). The dolomite component consists of a gastropod floatstone-rudstone with marginal section of a fusulinid foraminifera (white arrow). Note the incomplete sedimentary filling of the gastropod cavities with sparitic cement in the upper parts (grey arrow) recording the stratigraphic way up. The calcite marble shows evidence for dynamic recrystallization by bulging of 0.5 mm large calcite crystals (XPL, 492807E, 4099880N). f) Cataclastic quartz-rich schist strongly overprinted by dissolution-precipitation creep from the Telendos Thrust (XPL, 494233E, 4099758N). g) Ultramylonite from the Telendos Thrust. The thin section is from the same outcrop from which K35 was sampled for white mica $^{40}Ar/^{39}Ar$ dating from the cleavage domains (XPL + tint plate, 494281E, 4099770N). h) SCC' fabric from a shear zone (Telendos Thrust) within the amphibolites from the basement of the Marina Unit (XPL, 493822E, 4094101N).

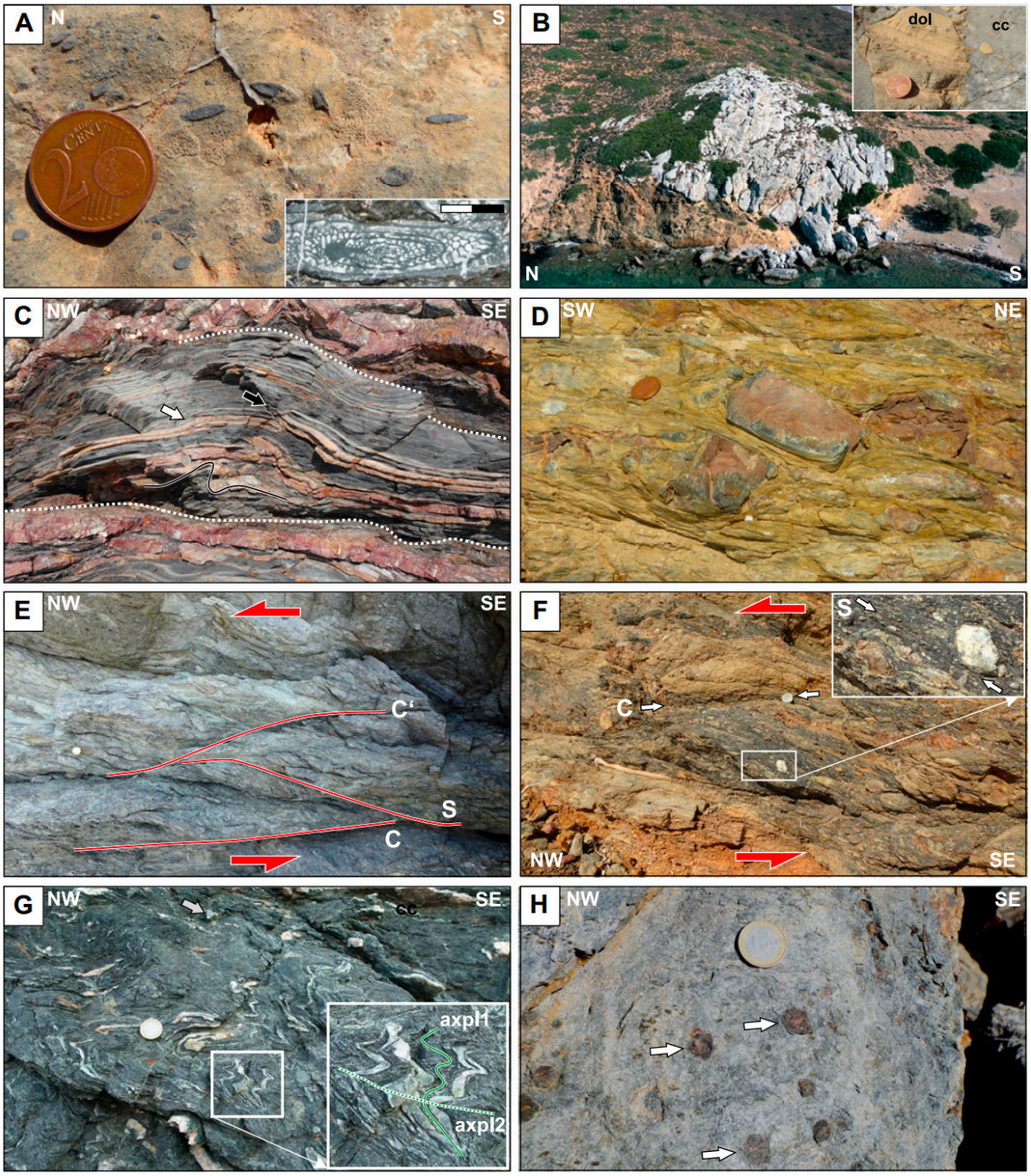

1354

1355 Figure 7: a) Fusulinid floatstone-rudstone with cystoporate bryozoans. Small insert picture shows a
1356 thin section of Pseudofusulinoides *sp.* Bedding plane (266/09) of dark marly limestone of the
1357 Kefala Unit with various sections through fusulinidae (492658E, 4099668N). Inset shows a thin
1358 section (scale bar indicates 1 mm). b) Drone picture of a large calcitic (cc) marble block (50 m
1359 diameter) within the wildflysch of the Kefala Unit (492698E, 4099923N, 20 m a.s.l.). The
1360 southern side of the block is composed of a calcitic marble conglomerate with isolated angular
1361 blocks of dolomite (dol) from cm- to several dm-size, which preserved sedimentary layering
1362 (inset; for a thin section see Fig. 6e). c) Soft sediment deformation in radiolarite layers in
1363 metapelites (wildflysch of the Kefala Unit) on Telendos (492572E, 4094846N). Shortening in the

radiolarite layers (mean dip direction 147/25) is accommodated along layer-parallel detachment horizons (white dotted lines). Note SE-vergent detachment folds (outlined with a black solid line, fold axis 055/15, axial plane 310/42) and NW-directed thrusting of individual radiolarite layers. Whereas both radiolarite layers are disrupted and thrusted at the location indicated by the black arrow, only the lower layer has been dislocated in between the two layers at the location indicated with the white arrow. d) In the wildflysch of the Kefala Unit, the radiolarites are reworked and appear as components in the conglomerates. A pressure-solution cleavage formed in the metapelitic matrix is wrapping around the apparently rigid blocks of radiolarite (493529E, 4099969N). e) Fault rock of the Telendos Thrust, which juxtaposes the amphibolites of the basement of the Marina Unit on top of the wildflysch of the Kefala Unit. Typically, the fault rock are cataclasites, which are strongly overprinted by dissolution-precipitation creep forming SC/SCC' fabrics (C 048/31, S 138/45 C' 328/14). The shear sense is top-to-NW. f) Black ultracataclasites with cm-scale well-rounded quartz clasts overprinted by dissolution-precipitation creep forming SC-type fabrics. The shear sense is top-to-NW (494281E, 4099770N). g) Polyphase folded amphibolites of the basement of the Marina Unit (493822E, 4094101N). Type-3 hook and crescent refold structures with a first axial plane (green solid line axpl1) folded by a common fold axis (mean 050/25) with a second axial plane (green dotted line axpl2). h) Quartz-mica schist in the basement of the Marina Unit with up to cm-scale garnets (493819E, 4092101N).

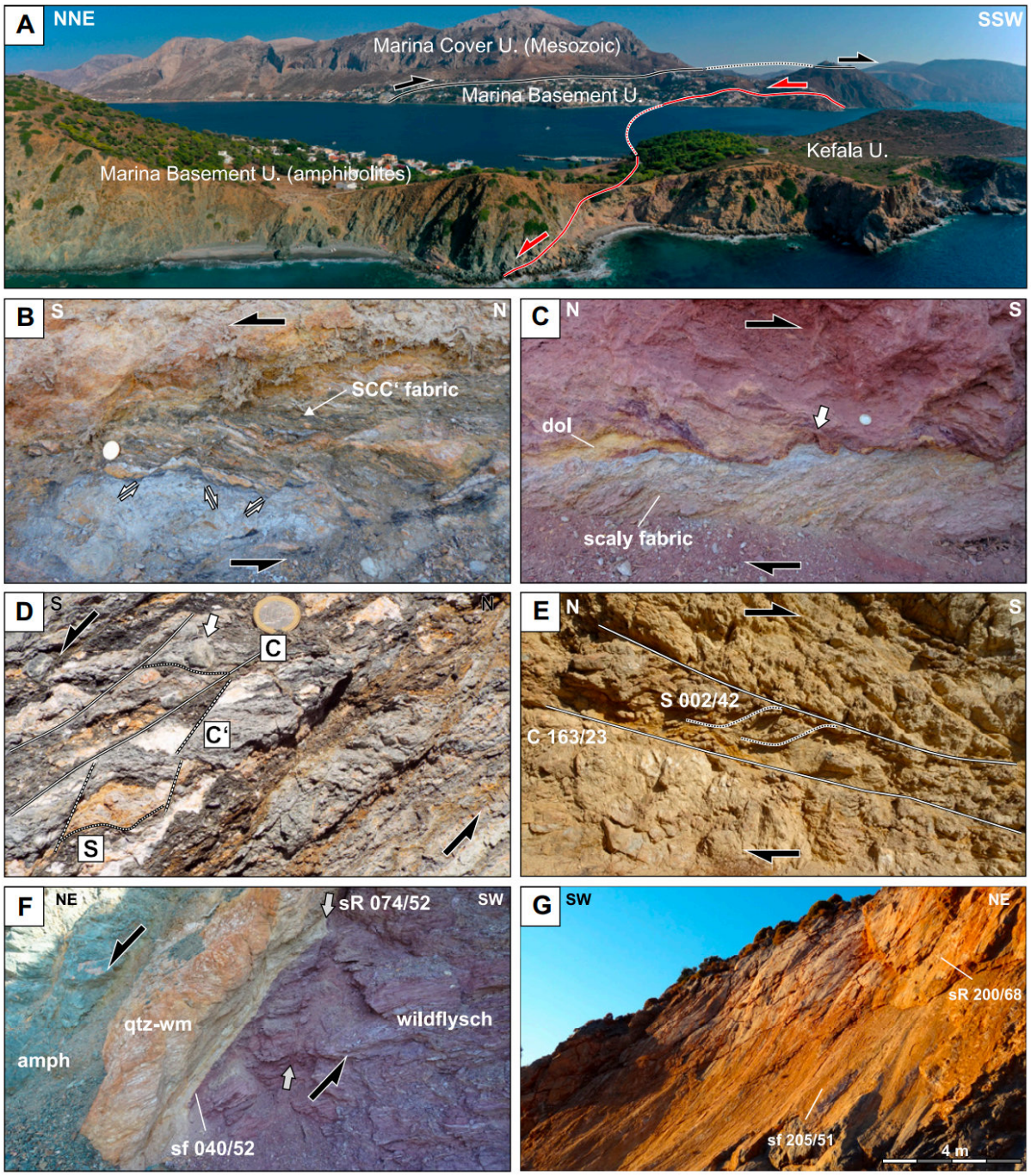

Figure 8: a) Drone picture of the southern parts of Telendos in the foreground and Kalymnos in the background (492555E, 4094604N, 60 m a.s.l.). Red line shows the trace of the Telendos Thrust juxtaposing the basement of the Marina Basement Unit on top of the Kefala Unit. Black line outlines the location of the Kalymnos Detachment displacing the Mesozoic limestones of the Marina Cover Unit on top of the Marina Basement Unit. b) Phyllonitized quartz-mica schists as part of the fault rocks of the Kalymnos Detachment (493779E, 4092861N). SCC' fabrics indicate ductile top-to-S shear sense, which is overprinted by a dominant set of brittle top-to-SSW (192/36) and a conjugate top-to-NNE (015/65) brittle fault set. c) Kalymnos Detachment localized in violet shales (Verrucano-type formation) at the base of the Mesozoic limestones of

the Marina Unit (496044E, 4098866N). The fault rocks consist of cataclastic shales with scaly fabrics, cataclastic yellow dolomite lenses (dol), ultracataclasites and fault gouges. Note the protrusions and injections of cataclasites into the fault gouges (white arrow). d) Kalymnos Detachment: multiple generations of foliated ultracataclasites and fault gauges, reworked by SC/SCC' fabrics indicating top-to-S shear sense (493741E, 4091950N). The mature cataclasites show up to 1 cm scale well rounded and partly polished clasts (white arrow). e) Top-to-SSE brittle-ductile shear zone with scaly fabrics in the conglomerates in the wildflysch of the Kefala Unit. f) Brittle high-angle fault (sf) offsetting the basement (amphibolite: amph, quartz-mica schists: qtz-wm) of the Marina Unit against the wildflysch (492756E, 4094605N). Synthetic Riedel faults (sR) confirm the normal displacement of the high angle faults. g) Brittle high-angle normal faults (sf) and synthetic Riedel faults (sR) in the Mesozoic limestones of the Marina Unit form the northern margin of the WNW-ESE striking graben at Arginonta (497959E, 4096540N).

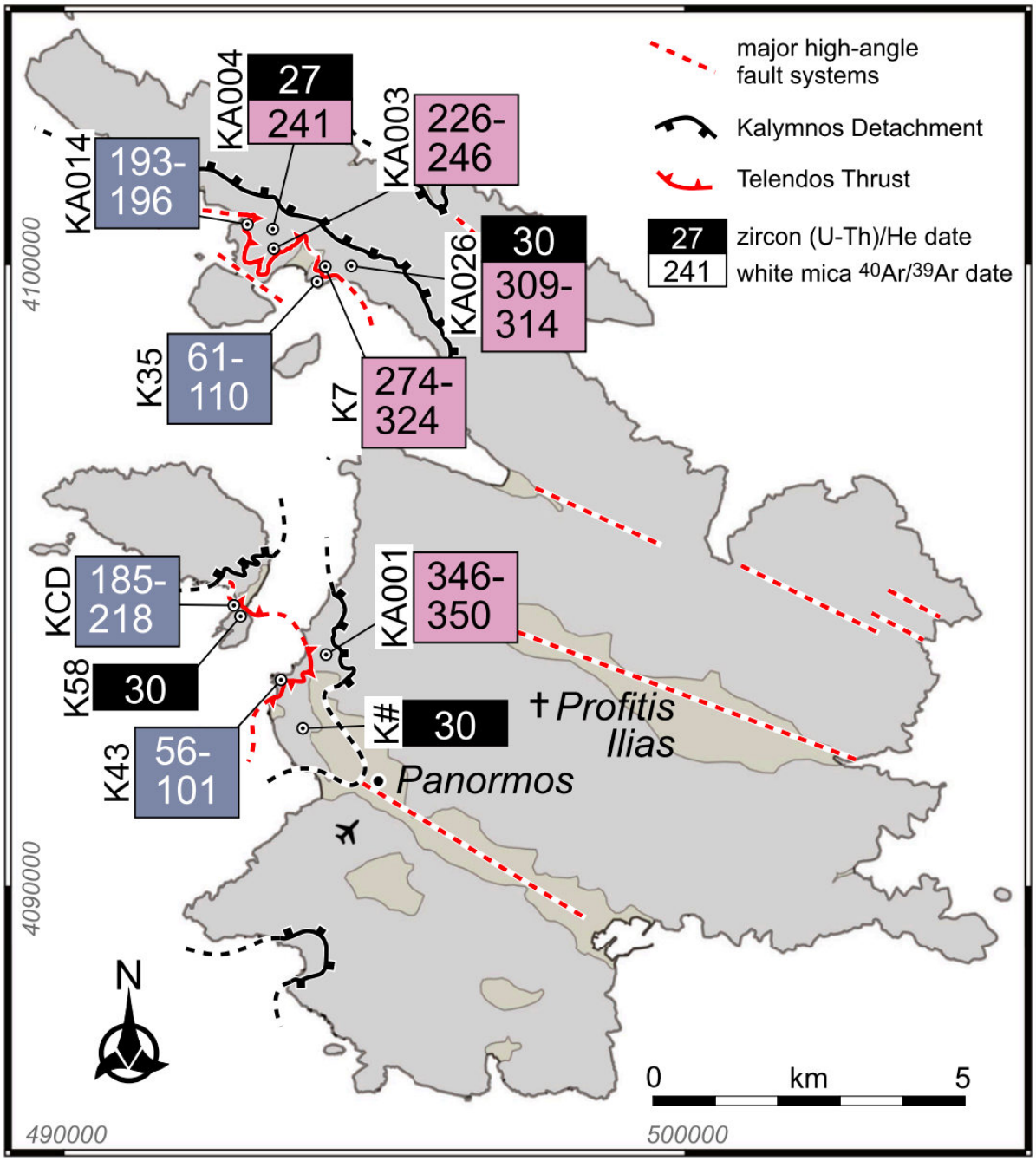

1405

1406 Figure 9: Map of Kalymnos with the major tectonic contacts. Blue-grey rectangles are white mica
1407 $^{40}Ar/^{39}Ar$ ages close to the Telendos Thrust. Dusky pink squares indicate white mica $^{40}Ar/^{39}Ar$
1408 ages from the Variscan basement. Black rectangles show zircon (U-Th)/He ages. See Table 1 for
1409 analytical data.

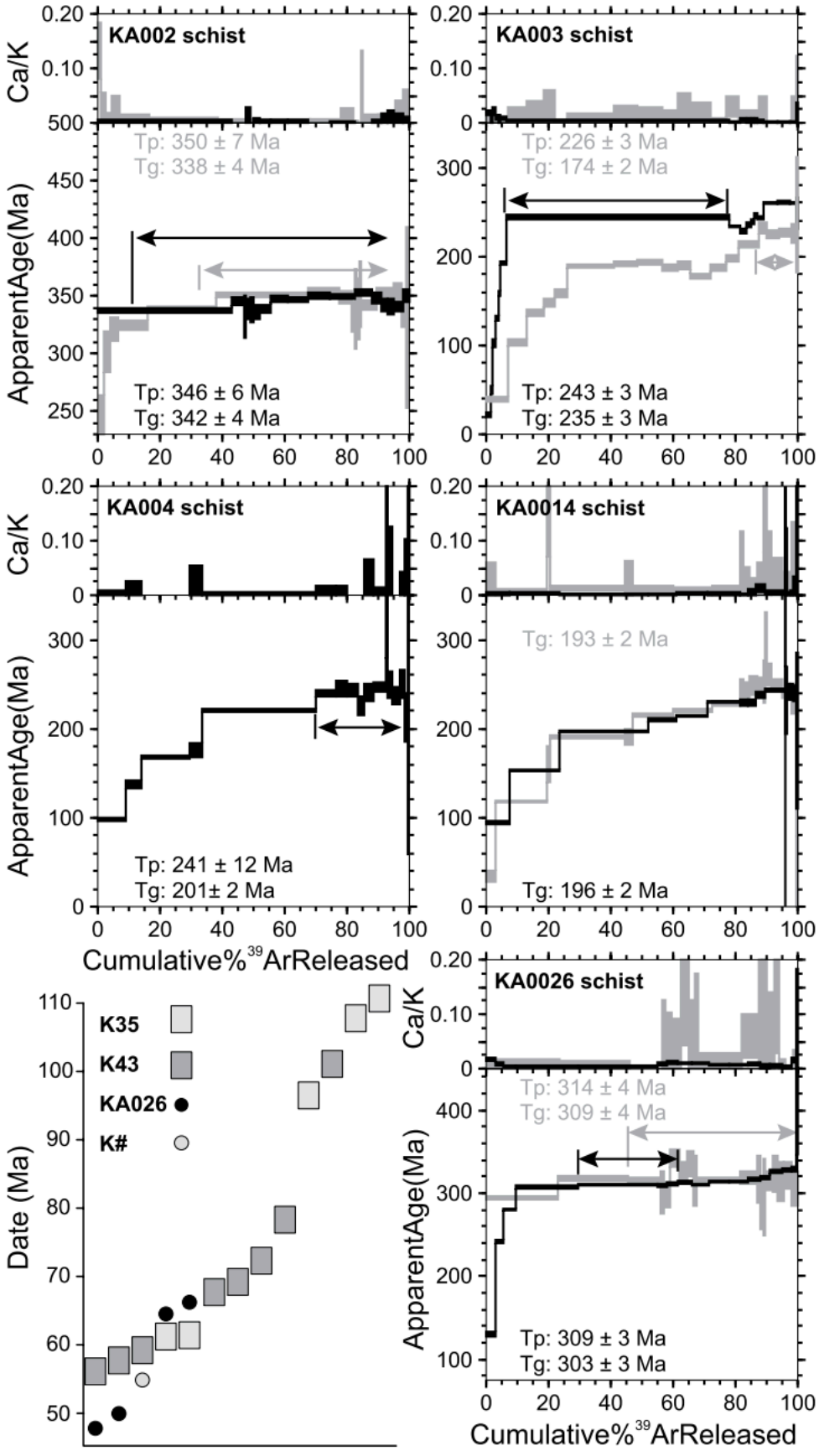

Figure 10: White mica $^{40}Ar/^{39}Ar$ age spectra from Kalymnos, Dodecanese, Greece. The width of each bar (thermal increment) represents the proportion of evolved gas, and the height represents

the uncertainty associated with the apparent age. Tg: total-gas integrated age. Tp: preferred age. Note the Apparent Age scale change between figures. Lower left graph highlights distribution of Late Cretaceous-Paleocene/Eocene single mica $^{40}Ar/^{39}Ar$ dates (squares) and single zircon (U-Th)/He dates (circles). See Figure 9 for sample locations, Table 2 for (U-Th)/He data, and the Supplementary Information Table S2 for $^{40}Ar/^{39}Ar$ data.

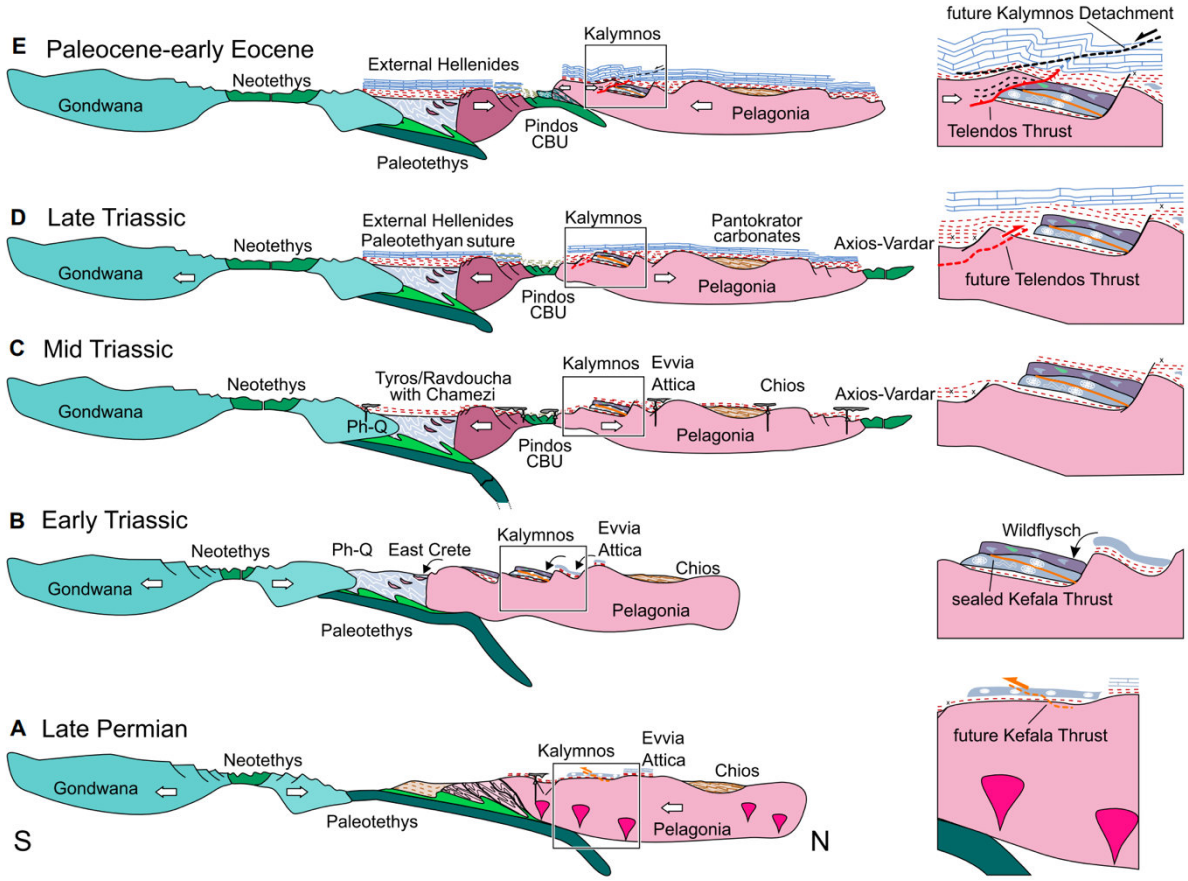

Figure 11: Schematic paleogeographic cross sections through the Aegean between the late Permian and Paleocene-early Eocene. Right column shows the details of Kalymnos as indicated by the rectangle in the cross sections. See text for a detailed description.

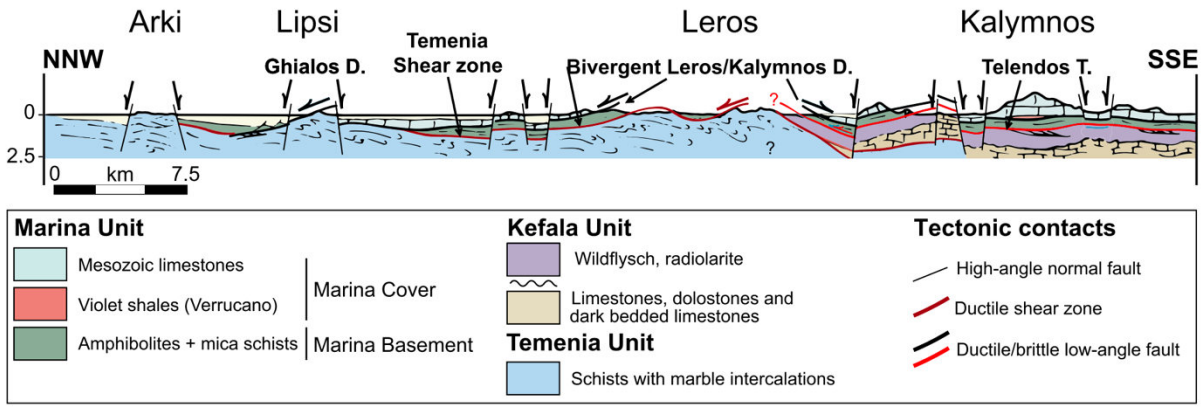

Figure 12: NNW-SSE oriented section across the northern and central Dodecanese showing the bivergent Ghialos/Leros and Kalymnos detachments (modified after Roche et al., 2018).

Table Captions:

Table 1: (Table 1. Zircon (U-Th)/He data (ages at 2s) from Kalymnos and Telendos islands, Dodecanese, Greece

Supplementary Information: geochronology methods

Table S1: $^{40}Ar/^{39}Ar$ isotopic data for white mica, Kalymnos and Telendos islands, Dodecanese, Greece

Table S2: $^{40}Ar/^{39}Ar$ isotopic data for white mica, Kalymnos and Telendos islands, Dodecanese, Greece